PNNL-14289

Pacific Northwest
National Laboratory
Operated by Battelle for the
U.S. Department of Energy

Geochemistry of Samples from Borehole C3177 (299-E24-21)

D. G. Horton
H. T. Schaef
R. J. Serne
C. F. Brown
M. M. Valenta
T. S. Vickerman
I. V. Kutnyakov
S. R. Baum
K. N. Geiszler
K. E. Parker

May 2003

Prepared for the U.S. Department of Energy
under Contract DE-AC06-76RL01830

DISCLAIMER

PACIFIC NORTHWEST NATIONAL LABORATORY
operated by
BATTELLE
for the
UNITED STATES DEPARTMENT OF ENERGY
under Contract DE-AC06-76RL01830

Printed in the United States of America

Available to DOE and DOE contractors from the
Office of Scientific and Technical Information,
P.O. Box 62, Oak Ridge, TN 37831-0062;
ph: (865) 576-8401
fax: (865) 576-5728
email: reports@adonis.osti.gov

Available to the public from the National Technical Information Service,
U.S. Department of Commerce, 5285 Port Royal Rd., Springfield, VA 22161
ph: (800) 553-6847
fax: (703) 605-6900
email: orders@ntis.fedworld.gov
online ordering: http://www.ntis.gov/ordering.htm


This document was printed on recycled paper.
(8/00)

PNNL-14289

Geochemistry of Samples from Borehole C3177 (299-E24-21)

D. G. Horton
H. T. Schaef
R. J. Serne
C. F. Brown
M. M. Valenta
T. S. Vickerman
I. V. Kutnyakov
S. R. Baum
K. N. Geiszler
K. E. Parker

May 2003

Prepared for
the U.S. Department of Energy
under Contract DE-AC06-76RL01830

Pacific Northwest National Laboratory
Richland, Washington 99352

Executive Summary

CH2M HILL Hanford, Inc., drilled the second borehole C3177 for the Immobilized Low-Activity Waste (ILAW) disposal site in 2001. The borehole is located just south of Fourth Street in the middle of the 200 East Area and in the northeast corner of the ILAW disposal site.

Vadose zone samples from that borehole were characterized by scientists from Pacific Northwest National Laboratory. The information from this characterization will be used to augment data previously collected to support future performance assessments of the ILAW facility.

The physical and geochemical properties were determined for six large composite samples and six discrete depth samples from the second ILAW borehole C3177. The composite samples were made so that large volumes of well characterized material can be used in future geochemical studies. These studies may help determine interactions between Hanford formation sediment and contaminants that may leach from the glass waste forms scheduled to be disposed in the ILAW facility.

All samples were analyzed for particle-size distribution, moisture content, whole sediment chemical composition, carbon content, surface area, mineralogy, pH, electrical conductivity, alkalinity, and the major and trace metal and anion concentrations of 1:1 sediment to water extracts.

This investigation determined that all composite samples are sand or gravelly sand. The moisture content ranges from 1.7 to 5.3 wt. %. The bulk chemistry and mineralogy of the samples are typical of the Hanford formation sand-dominated sequence. Likewise, the chemical characteristics of the 1:1 water extracts are similar to extracts from other samples of the Hanford formation sand-dominated sequence from other boreholes. The water extracts (and by inference the natural vadose zone pore water) from borehole C3177 are dominated by calcium, bicarbonate (from alkalinity), magnesium, sodium, and sulfate.

No information was found by this characterization effort that would invalidate any of the data used in the 2001 performance assessment (Mann et al. 2001) of the overall performance of the ILAW facility.

Contents

Figures

Tables

1.0 Introduction

This report contains the results of geochemical and physical property analyses of twelve samples from the Immobilized Low-Activity Waste (ILAW) borehole #2 (borehole name 299-E24-21; borehole number C3177).

Borehole C3177 was drilled in 2001 just south of Fourth Street in the middle of the 200 East Area and at the northeast corner of the ILAW disposal site. The borehole was drilled with a Becker hammer drill rig and near-continuous core was collected from 45 feet (ft) below ground surface (bgs) to total depth at 335 ft bgs. The drill core was retrieved in 2-ft-long plastic liners that were capped as soon as possible after being removed from the split tube sampler. Details of the drilling activities and the geologist's log are given in Walker (2001). Detailed descriptions of the drill core and the geologic interpretation are given in Reidel et al. (2001).

All drill cores were stored in refrigerators in the Pacific Northwest National Laboratory (PNNL) Applied Geology and Geochemistry laboratory in the 3720 Building until they were sampled.

English units are used in this report for descriptions and discussions of drilling activities and samples because that is the system of units used by drillers to measure and report depths and well construction details. To convert feet to meters, multiply by 0.3048; to convert inches to centimeters multiply by 2.54. The metric system is used in this report for all other purposes.

2.0 Samples

Twelve samples were selected from the core for detailed analyses. Table 2.1 lists the samples and gives a short description of each. Samples are identified by the borehole number followed by a depth (in ft bgs) suffix.

Two types of samples were collected: composite samples and discrete depth samples. The composite samples were made so that large volumes of well characterized material would be available for future studies. Six composite samples were made by combining and mixing several 2-ft sections of core. Each composite was homogenized in 5-gallon buckets before subsampling for analyses. Composite samples are identified in Table 2.1 along with the other six samples. The depths of drill cores used to make the composite samples are given in Table 2.2. Several kilograms of the characterized, composite samples remain for future studies.

Six depth discrete samples were collected from core to characterize specific features identified by the geologists during detailed examination (Reidel et al. 2001). The sample at 80.3-ft depth was collected to characterize a paleosol(1) identified by the geologist during description of the core in the laboratory. The paleosol was identified by the geologist at 78 ft bgs, whereas the sample collected for this effort was taken at 80.3 ft bgs. Thus, the sample used for this study probably represents the bottom of the paleosol or the sediment immediately below the paleosol.

The sample collected at 113.3 ft bgs represents a discrete, thin (~0.5-in.-thick) silt lens typical of silt lenses found in the Hanford formation sand-dominated sequence. The sample from 168.5 ft bgs is from the bottom of the R2 paleomagentic layer and represents a discrete sample of the Hanford formation sand-dominated, layer 2. (See Reidel et al. 2001 for the definition of the stratigraphy encountered in borehole C3177.) The sample from 170.4 ft bgs is the paleosol identified at that depth by Reidel et al. (2001) during core logging. The two samples from 223.5 and 242.0 ft bgs are from above and below the N1/R1 paleomagnetic boundary and were collected to characterize any differences above and below that contact.

Table 2.1. Samples Collected from Borehole C3177

Sample Number[a]	Description
C3177-45	Composite sample; Hanford formation Layer 3.
C3177-80.3	Sediment associated with a paleosol at the Hanford formation Layer 3/Layer 2 boundary; bedded, medium-grained sand; beds are distinguished by color and hardness.
C3177-110	Composite sample; Hanford formation Layer 2.
C3177-113.3	Silt lens in the Hanford formation Layer 2.
C3177-150	Composite sample; Hanford formation Layer 2.

(1) A paleosol is a buried soil horizon of the geologic past.

Table 2.1. (Cont.)

Sample Number[(a)]	Description
C3177-168.5	Hanford formation Layer 2; bedded, medium-grained sand with a trace of silt; sample is from the base of the R2 (paleomagnetic) layer.
C3177-170.4	Paleosol at the Hanford formation Layer 2/Layer 1 boundary; fine-grained sand to silt; bioturbated and bleached with calcite cement.
C3177-200	Composite sample; Hanford formation Layer 1.
C3177-215	Composite sample; Hanford formation Layer 1.
C3177-223.5	Hanford formation Layer 1; coarse-grained sand; slight reaction to HCl; bottom of the N1 (paleomagnetic) layer.
C3177-242.0	Hanford formation Layer 1; sandy gravel; near the top of the R1 (paleomagnetic) layer.
C3177-251	Composite sample; Hanford formation Layer 1.
(a) Sample numbers are the borehole designation followed by the depth below ground surface from where samples were collected. HCl = Hydrochloric acid.	

Table 2.2. Description of Composite Samples (modified from Reidel et al. 2001)

Sample Number	Depth (ft bgs) and Description
C3177-45	45 to 47 ft – 95 % coarse subangular sand; about 2% round pebbles up to about 4 cm; no cementation, no compaction; slightly silty; silt effervesces. 47 to 49 ft – From 47 ft to 48.5 ft is very coarse, subangular, salt and pepper sand with few sparse pebbles up to 7 mm; fining upward with subtle bedding. 40% basalt, 60% felsic; well sorted; some compaction; ~5% silt and 95% sand; silt effervesces, sand does not. 48.5 ft to 49 ft – Fine-to coarse-grained sand with subtle bedding; fining upward; at 49 ft is angular to subangular sand; 75% felsic, 25% basalt; some calcite grains. 50 to 52 ft – Very coarse-grained sand; subangular to subrounded, moist but not wet, no cementation or compaction. Some grains up to 2 to 3 mm; 30% basalt, 70% felsic. Minor silt that effervesces.

Table 2.2. (Cont.)

Sample Number	Depth (ft bgs) and Description
C3177-110	110 to 112 ft – Coarse-grained sand. 122 to 124 ft – 1.3-cm-thick fining upward beds defined by color; sand is subangular, 40% basalt and 60% felsic, well sorted, fairly compacted, and dry. No cement. Silt effervesces. 132 to 134 ft – From 132 ft to 132.6 ft is coarse-grained sand with minor 1.3- to 1.9-cm-thick beds. From 132.5 ft to 134 ft is coarse sand; 40% basalt and 60% felsic, angular to subangular, well-sorted, dry, very compact, and not cemented. Silt effervesces. Rare rounded, basalt pebbles about up to 7 mm in size and oxidized. 135 to 137 ft – 98% sand; laminated, fining upward beds that are about 5- to 2.5-cm thick. Sand is mostly coarse grained with some fine-grained sand. Minor pebbles up to 8 mm in size. Sand is 40% basalt and 60% felsic, subangular, well sorted, and slightly moist; no cementation but well compacted. Minor silt effervesces.
C3177-150	150 to 151 ft – Core contains layering defined by color banding. Medium-grained sand; 40% felsic and 60% basaltic, well sorted, subangular, slightly moist, and poorly compacted. Moderate reaction to HCl. 152 to 154 ft – From 152 ft to 152.5 ft is fine-grained sand. From 152 ft 6 in. to 153 ft 3 in. is a fining upward sequence of sand. From 153.4 ft to 154 ft is fine sand that is layered in 1.25- to 2.5-cm bands denoted by color; sand is well sorted, 40% basalt and 60% felsic, subangular, and well compacted with no cementation. Silt effervesces. Some basalt pebbles (less than 7 mm in size) in coarser sand.
C3177-200	200 to 201 ft – From 200 ft to 200.75 ft is a fine pebble unit that fines upward to coarse-grained sand; 50% basalt, 50% felsic. From 200.75 ft to 201 ft is fining upward coarse-grained sand; moderately well sorted, slightly moist, poorly compacted; 70% basalt and 30% felsic. Moderate reaction to HCl. 202 to 204 ft – Coarse-grained sand with 1 to 2% pebbles up to 10 mm in size. Sand is 50% basalt and 50% felsic. Pebbles and sand are subangular, slightly moist, moderately sorted, and slightly compacted. Minor silt; silt and sand effervesce.

Table 2.2. (Cont.)

Sample Number	Depth (ft bgs) and Description
C3177-215	215 to 216 ft – Coarse to very coarse sand. 217 to 219 ft – Color bedding based on basalt content. Lighter layers are 40% basalt and 60% felsic; darker layers are 60 to 70 % basalt and 30 to 40% felsic. Sand is coarse grained. Basalt rich layers are coarser with grains up to 3 to 5 mm and some as large as 10 mm. Sand is well sorted, slightly moist, and moderately compacted. Pebbles near bottom of core are up to 2 to 3 cm in size. Slight to moderate reaction to HCl. 230 to 231 ft – Pebbles and cobbles. 232 to 234 ft – Coarse-grained sand and fine-grained pebbles; poorly sorted, moderately compacted, 50 % basalt and 50% felsic. Sand is subangular and pebbles are rounded. Some basalt pebbles up to 3 cm. Moderate reaction to HCl.
C3177-251	251 to 252 ft – Medium- to coarse-grained sand. 260 to 261 ft – Medium- to coarse-grained sand; well sorted, subangular to subrounded, slightly moist, compacted but not cemented. No pebbles. Moderate reaction with HCl. 261.5 to 263.5 ft – Medium- to coarse-grained sand.
HCl = Hydrochloric acid.	

3.0 Analytical Methods

All analyses except x-ray fluorescence (XRF) and loss-on-ignition (LOI) were preformed in the Applied Geology and Geochemistry laboratories at PNNL. XRF and LOI analyses were done at Washington State University's GeoAnalytical laboratory in Pullman, Washington. All original analytical data along with associated quality control (QC) data can be obtained from the laboratory that performed the analyses.

3.1 Particle Size Distribution

The wet sieving and hydrometer methods were used to determine the particle-size distribution for each of the composite samples. The techniques are based on the American Society for Testing and Materials procedure *Standard Test Method for Particle-Size Analysis of Soils* (ASTM Method D422-63). The resulting clay-size fractions were saved for mineralogical analyses.

3.2 Moisture Content

Gravimetric water contents of the 12 samples were determined using PNNL procedure PNL-MA-567-DO-1 (PNL 1990). This procedure is based on the American Society for Testing and Materials procedure *Test Method for Laboratory Determination of Water (Moisture) Content of Soil, and Rock* (ASTM D2216-98). One representative subsample of at least 15 to 70 grams (g) was taken from each sample for the analyses. Samples were placed in tared containers, weighed, and oven dried at 105°C until constant weight was achieved, which took at least 24 hours. The containers then were removed from the oven, sealed, cooled, and weighed. At least two weighings, after 24 hours of drying, were done to ensure that all moisture was removed. All measurements were made with a calibrated balance. Calibrated weights were used to verify balance performance. The gravimetric water content was computed as percentage change in soil weight before and after oven drying.

3.3 X-ray Fluorescence

The elemental composition of the bulk sediment was determined by XRF using analytical and sample preparation methods developed by Washington State University. The following description of the method is abstracted from the Washington State University laboratory's web page at http://www.wsu.edu:8080/~geology/Pages/Services/DJ_Paper/DJPaper.html.

Approximately 28 g of each sample were ground in a swing mill with tungsten carbide surfaces for two minutes. A powder sample of 3.5 g was weighed into a plastic mixing jar with 7 g of spectroscopically pure dilithium tetraborate ($Li_2B_4O_7$) and, assisted by an enclosed plastic ball, mixed for ten minutes. The mixed powders were emptied into graphite crucibles and placed on a silica tray before being loaded into a muffle furnace. Fusion generally occurred within five minutes from the time the preheated furnace returned to its normal 1,000°C after loading. The silica plate and graphite crucibles were then removed from the oven and allowed to cool. Each bead was reground in the swing mill for 35 seconds; the glass powder was then returned to the graphite crucibles and refused for five minutes.

Following the second fusion, the lower flat surface of each bead was ground on 600 silicon carbide grit, finished briefly on a glass plate (600 grit with alcohol) to remove any metal from the grinding wheel, washed in an ultrasonic cleaner, rinsed in alcohol, and wiped dry.

The concentrations of 27 elements in the unknown samples were measured by comparing the x-ray intensity for each element with the intensity for two beads each of nine U.S. Geological Survey standard samples (PCC-1, BCR-1, BIR-1, DNC-1, W-2, AGV-1, GSP-1, G-2, and STM -1), using the values recommended by Govindaraju (1994) and two beads of pure vein quartz used as blanks for all elements except silicon. In the laboratory, the 20 standard beads are run and used for recalibration approximately once every three weeks or after the analysis of about 300 unknowns. The intensities for all elements were corrected automatically for line interference and absorption effects due to all the other elements using the fundamental parameter method. The spectrometer operating conditions used can be found on the Washington State University web page cited in the first paragraph of this section.

3.4 Loss-On-Ignition

LOI also was determined by the Washington State University GeoAnalytical laboratory as part of the XRF process. LOI was determined to account for volatile components lost during the fusion of the XRF samples. LOI was determined by firing 9 to 10 g of sample at 900°C for 16 hours.

3.5 Carbon Content

The total carbon concentration in each sample was determined using the procedure *Standard Methods for Total and Organic Carbon in Water by High Temperature Oxidation and by Coulometric Detection* (ASTM Method D4129-88). Total carbon was measured with a Coulometrics, Inc., Model 5051 Carbon Dioxide Coulometer with combustion at approximately 980°C. Ultrapure oxygen was used to sweep the combustion products through a barium-chromate catalyst tube for conversion to carbon dioxide. Evolved carbon dioxide was quantified through coulometric titration following absorption in a solution containing ethanolamine.

Samples used for determining the total carbon content were placed into precombusted, tared platinum combustion boats and weighed on a four-place analytical balance. After the combustion boats were placed into the furnace introduction tube, a 1-minute waiting period was allowed for ultrapure oxygen carrier gas to purge any carbon dioxide introduced into the system during sample placement. The samples then were moved into the combustion furnace for titration. Sample titration readings were performed at 3 minutes after combustion began and again once stability was reached, usually within the next 2 minutes. The system background was determined by performing the entire process using an empty, precombusted platinum boat. Reagent grade calcium carbonate was used as a standard.

Inorganic carbon concentrations were determined using a Coulometrics, Inc., Model 5051 Carbon Dioxide Coulometer. A weighed aliquot of each sample was placed into acid-treated glass tubes. Following placement of sample tubes into the system, a 1-minute waiting period allowed the ultrapure oxygen carrier gas to purge carbon dioxide introduced to the system from the atmosphere. Inorganic carbon was released through acid-assisted evolution (50% hydrochloric acid) with heating to 200°C.

Samples were completely covered by the acid to allow full reaction to occur. Sample titration readings were performed 5 minutes following acid addition and again once stability was reached, usually within 10 minutes. Reagent grade calcium carbonate was used as a standard. Background values were determined.

Organic carbon was calculated by subtracting the inorganic carbon concentration from the total carbon concentration.

3.6 Mineralogy

The mineralogy of the bulk sediment and clay-size fractions of the samples was determined by standard, powder x-ray diffraction (XRD) techniques. The bulk samples were prepared by grinding 2 g of homogenized sample in a tungsten carbide ball mill grinder for 10 minutes. The milled powders were then packed into aluminum sample holders for analysis.

Approximately 100 g of sample were used for XRD analysis of the clay fractions. Each 100-g aliquot was mixed with 1.0 L of 0.001 M sodium hexametaphosphate and shaken overnight. The sand fraction was separated from the dispersed sample by wet sieving through a # 230 sieve (0.0625 mm). The silt fraction was separated from the clay fraction by Stoke's Law settling. The lower limit of the silt fraction was taken at 1.4 μm.

Each clay suspension was concentrated to an approximate volume of 30 milliliters (ml) by adding a few drops of 10 N $MgCl_2$ to the dispersed slurry. The amount of clay in the concentrated suspension was determined by drying a known volume of the suspension and weighing the dried sediment. Aliquots of slurry containing 250 mg of clay-size material were saturated with either 1 N $MgCl_2$ or KCl solutions.

Clay-size specimens were prepared for analysis using the aluminum alide method described by Drever (1973). Because the Mg^{2+} specimens tended to curl and peel off the slide, they were immediately solvated with a few drops of a 10% solution of ethylene glycol in ethanol and placed in a dessiccator containing excess ethylene glycol for a minimum of 24 hours. Potassium-saturated slides were air dried and analyzed, then heated to 550°C for 1 hour and re-analyzed.

All samples were analyzed on a Scintag XRD unit equipped using monochromated Cu K_α radiation (wavelength 1.5418 Å). Randomly oriented whole sediment samples were scanned from 2° to 65° 2θ with a dwell time of 14 seconds. Preferentially oriented clay-size specimens were scanned from 2° to 45° 2θ with a dwell time of 2 seconds. Scans were collected electronically and processed using commercial software (JADE® XRD pattern processing software). Mineral identification was based on powder diffraction files published by the Joint Committee for Powder Diffraction Standards (1974).

Semi-quantification of minerals in the bulk sediments were determined using the whole pattern fitting technique provided by the JADE® XRD pattern processing software. The software fits a diffraction model to the analytical data by non-linear least-square optimization in which crystallographic parameters are varied to improve the fit between the two patterns. Success of the refinement process is measured by a ratio of the weighted and calculated errors. This value, referred to as "goodness of fit", is expected to be close to one in an ideal refinement.

Mineral abundances in the <1.4 μm fraction were determined using the method of external standards described in Brindley (1980). Pure mineral phases of illite, smectite, kaolinite, and chlorite were obtained from the Clay Mineral Society's Source Clays Repository, (The Source Clays Repository, The Clay Minerals Society, Purdue University, 915 West State Street, West Lafayette, IN 47907-2054). The reference minerals were analyzed under the same conditions as the sediment samples. Based on previous data collected from Hanford formation sediments (Serne et al. 2002a), an average mass absorption of 55 cm^2g^{-1} was assumed for the clay samples. Mass absorption values for the reference minerals were calculated from published chemical data (Newman and Brown 1987).

3.7 Surface Area

Surface area was measured with a Micrometrics Surface Area Analyzer, (Model 2010 Micrometrics Instrument Corp., Norcross, Georgia). The approach is based on the multi-point BET (Brunauer et al. 1938) adsorption equation using nitrogen. A detailed description of the procedure to determine surface area is presented in the operating manual supplied with the instrument. Briefly, an air-dried sediment sample, which will provide at least 10 m^2 of total surface area, is placed in a surface area flask and out gassed for a minimum of 3 hours at 150°C and at 3 μm Hg pressure. The out gassing temperature was chosen to minimize altering the surface structure as discussed by Davis and Leckie (1978). To determine dryness, the vacuum pumps were isolated using the "check" function on the instrument and if a vacuum change of less than 2 μm Hg in 5 minutes occurred, the sample was considered dry. After out gassing, the adsorption of nitrogen then determines the surface area on the surface.

The equipment uses an imbalance of atomic forces on the surface of a clean evacuated solid to attract gas molecules. The gas molecules collide with the surface of the sediment and either bounce off or adsorb onto the surface. When the molecules leave the bulk gas to adsorb onto the sediment surface, the number of molecules in the gas decreases; thus, the gas pressure decreases. The number of molecules adsorbed can be determined by knowing the temperature, volume of the container, and change in pressure. From the number of adsorbed molecules, the surface area can be calculated.

Both the bulk sediment and the clay-size fractions for the composite sediments were characterized to determine the BET surface area. Because the instrument glassware has a narrow neck (~0.9 cm inner diameter), particles larger than ~7 mm can't be placed into the apparatus. For some of the sediment samples, gravel particles larger than 7 mm were excluded from the aliquots used to measure bulk sediment surface area.

3.8 1:1 Sediment-to-Water Extract

Water soluble inorganic constituents were extracted from the sediment samples to characterize the amounts of water soluble ions in the samples. The water-soluble constituents were obtained from the samples using a 1:1 sediment-to-deionized-water extract method. This method was used because the sediment was too dry to easily extract vadose zone porewater. The extracts were prepared by adding enough deionized water to approximately 60 to 80 g of sediment sample to effectively get a 1:1 weight ratio. The weight of deionized water needed was calculated based on the weight of the field-moist samples and their previously determined moisture contents. The appropriate amount of deionized water

(enough to make the sum of deionized water and existing porewater equal the oven dry weight of the sediment) was added to screw cap jars containing the sediment samples. The jars were sealed and briefly shaken by hand, then placed on a mechanical orbital shaker for 1 hour. The samples were allowed to settle until the supernatant liquid was fairly clear, generally overnight. The supernatant was carefully decanted and separated into unfiltered aliquots for electrical conductivity and pH determinations, and filtered aliquots (passed through 0.45 μm membranes) for anion, cation, and dissolved inorganic carbon analyses. More details can be found in Rhoades (1996).

3.8.1 pH and Electrical Conductivity

Two approximately 3-ml aliquots of the unfiltered 1:1 water extract were used for pH and electrical conductivity measurements. The pH for the extracts was measured with a solid-state pH electrode and a pH meter calibrated with pH 4, 7, and 10 buffers. Electrical conductivity was measured and compared to potassium chloride standards with a range of 0.001 M to 1.0 M.

3.8.2 Alkalinity (Dissolved Inorganic Carbon)

Alkalinity was determined from the 1:1 water extracts using a standard titration with acid method. The alkalinity procedure is equivalent to the U.S. Geological survey method in the *National Field Manual for the Collection of Water-Quality Data* (USGS 2001).

3.8.3 Metals and Trace Metals

The concentrations of major metals in the 1:1 water extracts was determined with a Perkin Elmer Optima 3300 inductively coupled plasma optical emission spectrometer (ICP-OES) using high-purity calibration standards to generate calibration curves and verify continuing calibration during the analyses. Details are found in U.S. Environmental Protection Agency (EPA) Method 6010 (EPA 1986).

A thermoelemental PQ2 inductively coupled plasma mass spectrometer (ICP-MS) was used to analyze trace metals concentrations, including concentrations of technetium-99 and uranium-238. The analytical procedure is modeled on EPA Method 6020 (EPA 1986).

3.8.4 Anions

The 1:1 water extracts were analyzed for anion concentrations using a Dionex DX600 ion chromatograph. Carbonate, chloride, fluoride, nitrate, phosphate, and sulfate were separated on a Dionex AS17 column with a gradient elution of 1 mM to 35 mM NaOH and measured using a conductivity detector. The analytical method is based on EPA Method 300.0A (EPA 1993) with the exception of using the gradient elution with sodium hydroxide.

3.9 Iron Extractions

A series of iron extraction experiments were conducted using ILAW borehole composite samples C3177-45, C3177-110, and C3177-200 to investigate the fraction of extractable iron-oxides present. Four chemical extraction methods were examined to assess their effectiveness at targeting amorphous versus

crystalline iron-oxide phases (Anderson and Jenne 1970; Tessier et al. 1979; McAlister and Smith 1999; and Dong et al. 2000). All solutions used in the extraction procedures were prepared using reagent grade materials in double deionized water. Two methods, which utilize 10.9 g/L oxalic acid with 16.1 g/L ammonium oxalate at pH 3 or 0.04 M hydroxylamine hydrochloride in 25% (v/v) acetic acid as the extraction solution, are reported to solely extract amorphous iron-oxides (Tessier et al. 1979; Dong et al. 2000). The two methods that are reported to target all iron oxide solids employ either 0.3 M sodium dithionite with 0.175 M sodium citrate and 0.2 M sodium bicarbonate or 0.3 M sodium dithionite with 0.175 M sodium citrate and 0.025 M citric acid as the extractant (Anderson and Jenne 1970; and McAlister and Smith 1999).

Duplicate reaction vessels were prepared by weighing approximately 5 g of soil (on a dry-weight basis) into 250 ml Nalgene® centrifuge bottles. The soil samples were initially contacted with 40 ml of 1 M sodium acetate (brought to pH 5 with acetic acid) at room temperature for 1 hour to remove discrete carbonate solids and carbonate coatings from the soil. After the appropriate reaction time, the samples were centrifuged at 2,000 revolutions per minute (rpm) for approximately 30 minutes. The sodium acetate solution was decanted and the soil pellets were washed with 20 ml of double deionized water for 15 minutes, followed by the same centrifugation and decantation process. Duplicate sets of the washed soil samples were then extracted via one of the following four extraction processes: the oxalic acid/ammonium oxalate extraction was performed at a 1:40 solid-to-solution ratio for 4 hours (in the dark) at room temperature; the hydroxylamine hydrochloride extraction was conducted at a 1:20 solid-to-solution ratio for 6 hours at approximately 96°C; the two sodium dithionite extractions were performed at a 1:20 solid-to-solution ratio for 4 hours at 85°C. Once the reaction was complete, the samples were centrifuged at 2,000 rpm for approximately 30 minutes and the extraction solutions were decanted. An aliquot of each extraction solution was preserved with concentrated nitric acid (to a final nitric acid concentration of 1%) and analyzed for major cations via ICP-OES.

3.10 Cation Exchange Capacities

Several experiments were conducted using samples from borehole C3177 to investigate the total cation exchange capacity (CEC) of the borehole sediments as a function of depth. Three radio-tracer methods (^{22}Na, ^{85}Sr, and ^{137}Cs) were evaluated to determine their effectiveness and adaptability to measuring soil cation exchange capacities via column flow-through tests (Beetem et al. 1962; Babcock and Schulz 1969; Routson et al. 1973). Batch tests are typically chosen as the preferred experimental method due to their simplistic approach; however, they can lead to underestimation of the total sediment CEC due to loss of fine-grained material during the repeated washing/rinsing steps. Conversely, all sediment rinsing/washing is performed in-situ during column experiments, thereby eliminating the potential to wash away fine-grained materials. The aforementioned radio-tracer techniques will also be used to investigate the impact of divalent (Sr) versus monovalent (Na and Cs) cation substitution in sediments composed of a mixture of multivalent cations.

All solutions used in the CEC procedures were prepared using reagent grade materials in double deionized water. All three radio-tracer procedures required approximately 2 g of sample and were performed in Bio-Rad® poly-prep chromatography columns. The first step required slowly saturating the soil (approximately 50 ml/g) with a high ionic strength salt; 1.5 M sodium chloride, 0.5 M cesium

chloride, or 0.5 M strontium chloride for the ^{22}Na, ^{137}Cs, and ^{85}Sr methods, respectively. Next, the soil was equilibrated (approximately 50 ml/g) with low ionic strength solutions (0.04 M NaCl, 0.04 M CsCl, or 0.04 M $SrCl_2$, respectively) in preparation of the isotope exchange step. This was followed by three 3-ml rinses of the soil using the respective low ionic strength salt solutions containing at least 5,000 counts per minute (CPM) of the appropriate radio-isotope for the given salt base (i.e. ^{22}Na, ^{137}Cs, or ^{85}Sr). An aliquot of the final rinse was retained for gamma energy analysis (GEA) and final measurement of stable cation concentrations for the low ionic strength solutions. The final step involved rinsing the soil samples with three 3-ml aliquots of ethanol, followed by collection of the soil sample for analysis via GEA.

The total CEC of the soil (meq/g) was calculated by dividing the column activity per unit weight of soil (cpm/g) by the specific activity of the equilibration solution (cpm/meq).

4.0 Results and Discussion

This section presents the analytical results and interpretations of the results. The complete results for XRD, ICP-MS, ICP-OES, iron oxide extraction, and CEC analyses are listed in Appendix A. Cation anion balances and comparisons of calculated sulfate concentrations (from ICP-OES analysis for sulfur) with sulfate concentrations measured by ion chromatography have been made to check the internal consistency of the data set. The data and results of these consistency checks are presented in Appendix B.

4.1 Particle Size Distribution

Figures 4.1 to 4.6 show the data on particle-size distribution as determined by the wet sieve/ hydrometer method, for the six composite samples. The data show that most of the samples have a median grain size of about 0.5 to 0.6 mm. Sample C3177-251 (Figure 4.6) has the largest median grain size (about 1.5 mm) and sample C3177-150 (Figure 4.3) has the smallest median grain size (about 0.3 mm). All the samples are dominated by sand and moderately well sorted but none are very well sorted, reflecting the fact that they are composites of several feet of core over relatively long intervals. Sample C3177-150 (Figure 4.3) is the best sorted, as seen by the steepness of the mid-portion of the curve and relatively short tails, and this sample was made of only 3 ft of core distributed over only 4 ft of stratigraphic interval.

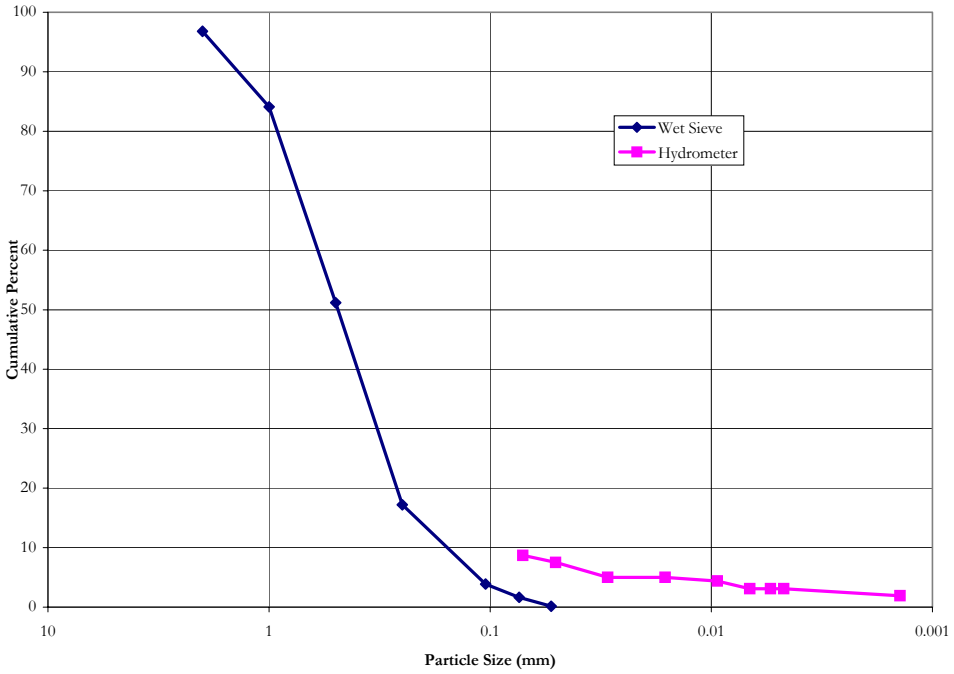

Figure 4.1. Particle-Size Distribution for Composite Sample C3177-45

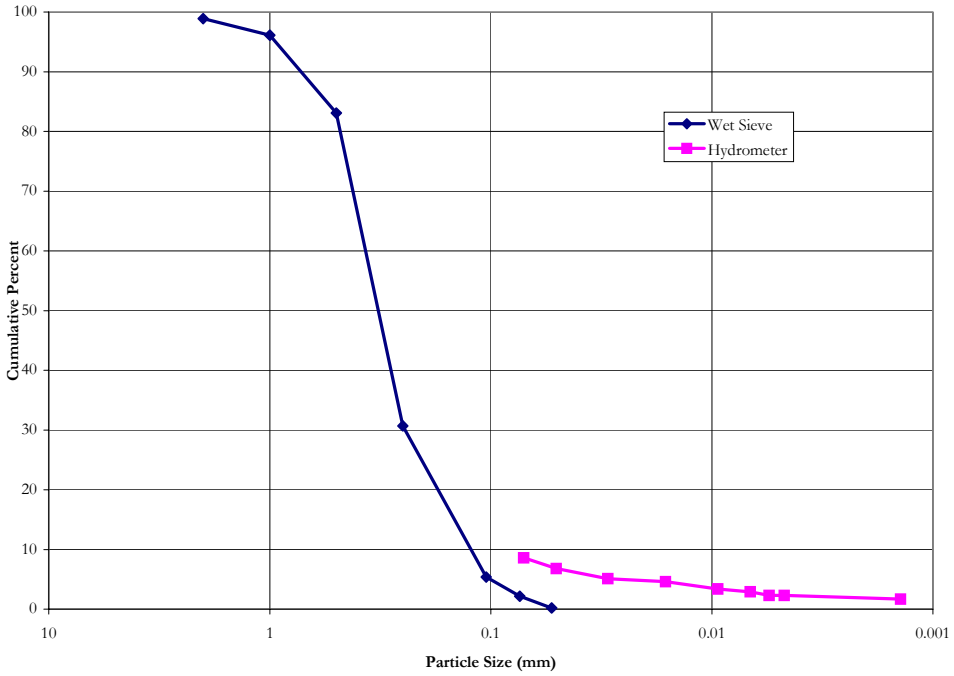

Figure 4.2. Particle-Size Distribution for Composite Sample C3177-110

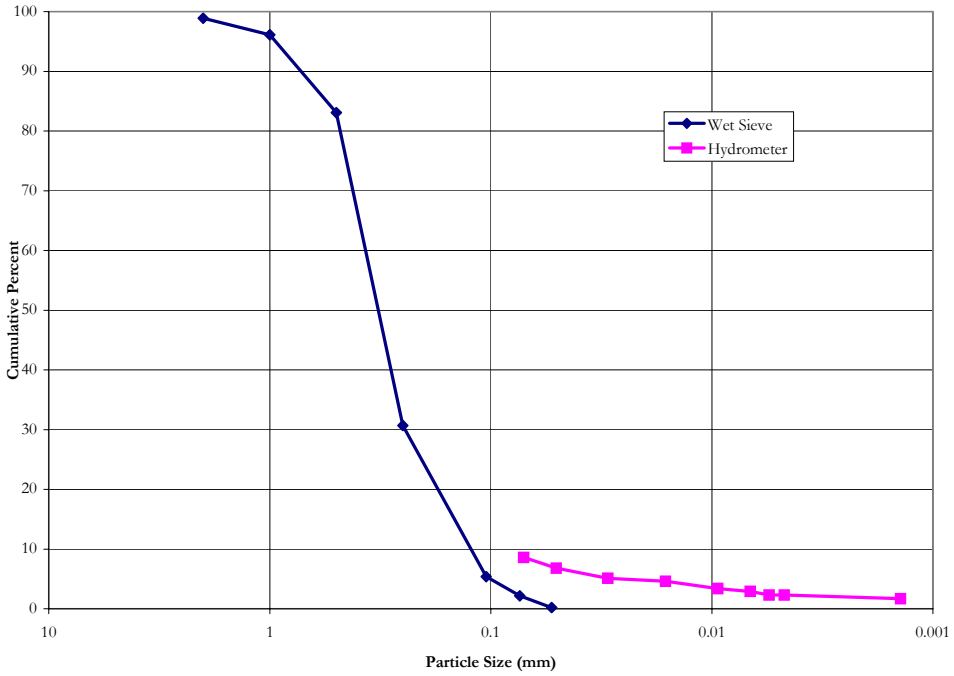

Figure 4.3. Particle-Size Distribution for Composite Sample C3177-150

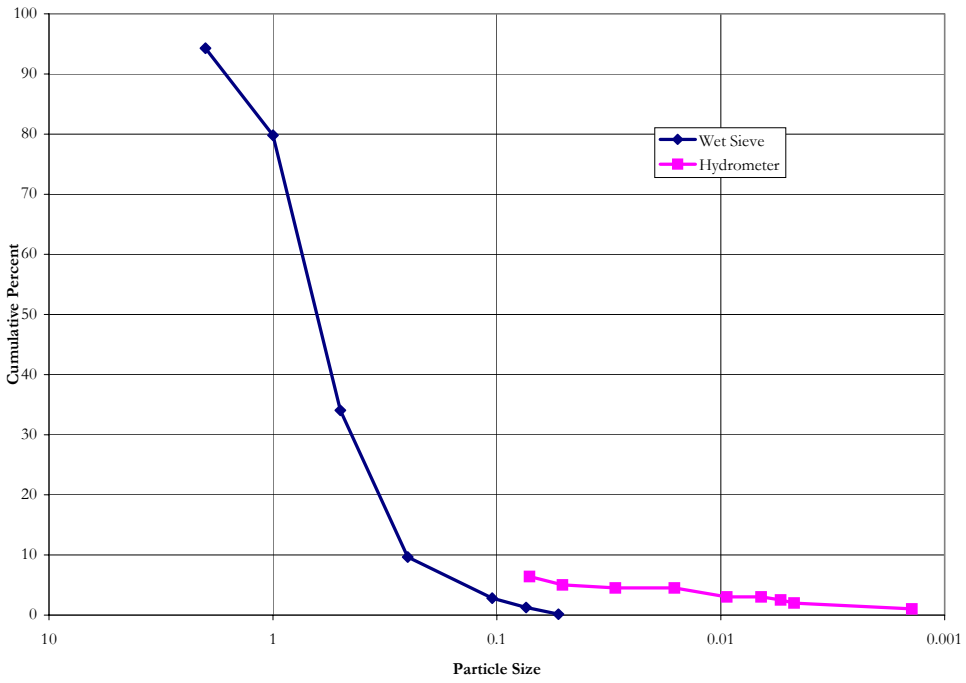

Figure 4.4. Particle-Size Distribution for Composite Sample C3177-200

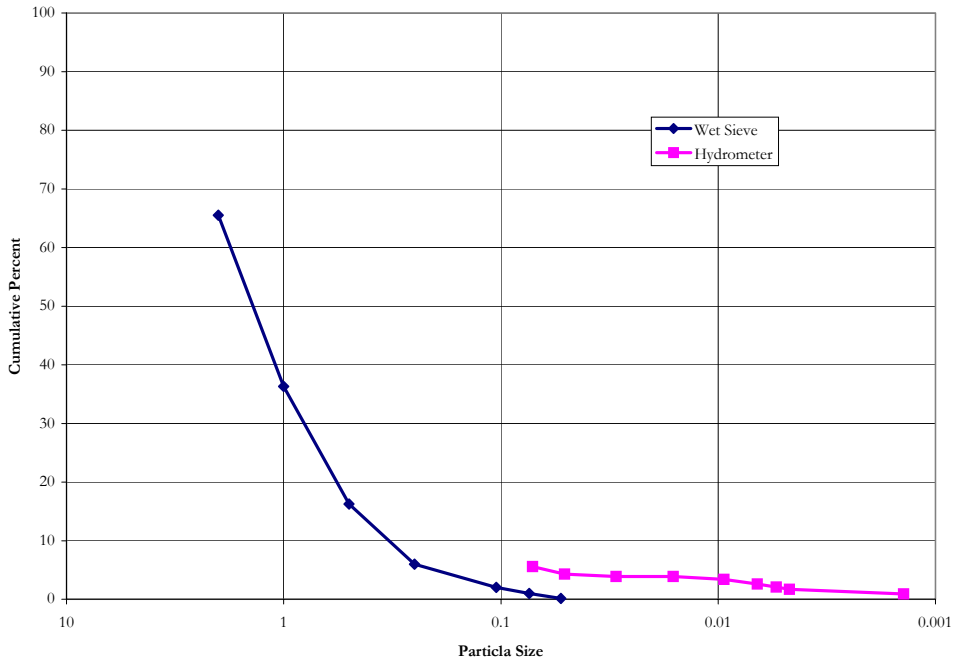

Figure 4.5. Particle-Size Distribution for Composite Sample C3177-215

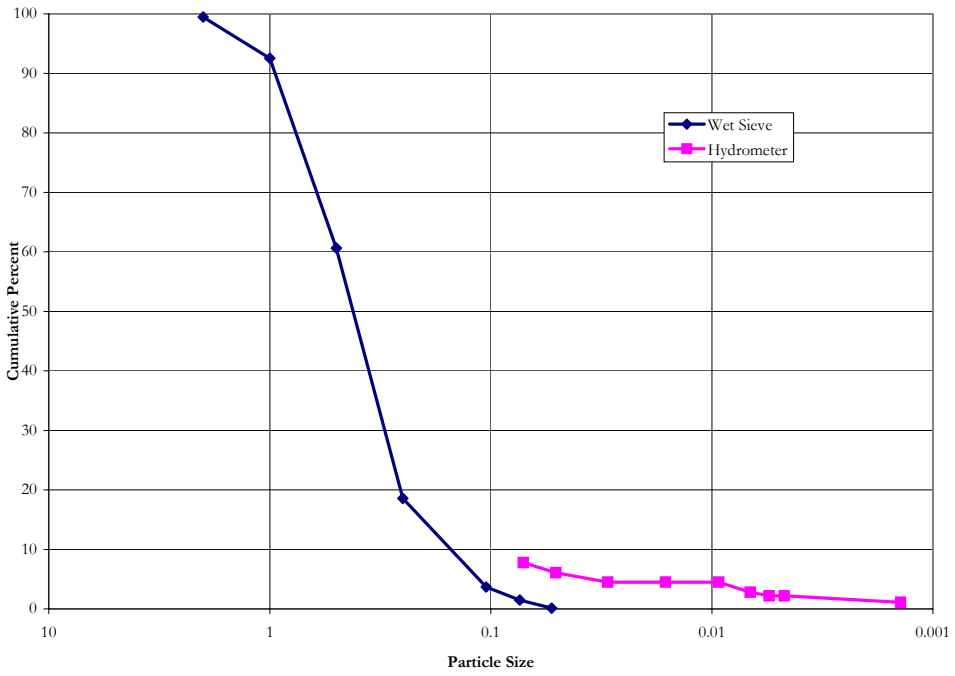

Figure 4.6. Particle-Size Distribution for Composite Sample C3177-251

The wet sieve data and the hydrometer data in Figures 4.1 to 4.6 do not line up perfectly. This is, in part, because the two methods measure two different aspects of the sample. The wet sieve method measures the amount of material smaller than a specific diameter. The hydrometer data measures the average diameter remaining in suspension. The differences between the two curves are not great and are not expected to affect future performance assessments of the site.

Table 4.1 gives particle-size distribution information along with the modified Folk-Wentworth (Folk 1968; Wentworth 1922) classification for each composite sample. None of the samples contain

Table 4.1. Summary of Particle-Size Distributions as Determined by Wet Sieve/Hydrometer Method (Normalized to 100 %) for Composite Samples from Borehole C3177

Sample Number	% Gravel	% Sand	% Silt	%Clay	Classification
C3177-45	1.05	92.16	5.41	1.38	Sand
C3177-110	3.85	88.60	6.19	1.36	Sand
C3177-150	1.27	91.60	6.12	0.99	Sand
C43177-200	5.25	89.36	4.44	0.94	Slightly gravelly sand
C3177-215	22.94	73.12	3.20	0.74	Gravelly sand
C3177-251	0.60	93.31	5.28	0.80	Sand

significant fine-grained particles (silt plus clay) and only two samples contain significant gravel. The data on particle-size distribution indicate that all of the composite samples are typical of the Hanford formation sand-dominated sequence (Serne et al. 2002a).

4.2 Moisture Content

The moisture content of all samples is shown in Table 4.2. The two paleosols and the silt lens samples have the highest moisture content. This reflects the fine-grained nature of these types of samples. Although the moisture content of the composite samples is within the known range for the Hanford formation, the values, especially those less than 2 wt % moisture are at the low end of the range. For the Hanford formation H2 sequence (sand sequence), Serne et al. (2002a) found no moisture content less than 2.2 wt. % in samples from two clean boreholes at WMA S-SX and none less than 2.5 wt. % in clean borehole 299-E33-338 at the southeast corner of 241-B Tank Farm. Probably, the composite samples partially dried in the laboratory during the homogenization process. Also, the values for the paleosols and silt lens seem low compared with other similar samples; thus, we suspect that drying also occurred during the processing of these fine-grained sediments.

Table 4.3 shows the results of moisture analyses from samples of borehole C3177 that were obtained immediately upon opening the cores for purposes of recharge studies. The data are presented here for comparison with data collected for this characterization effort that occurred several months after the geologic and recharge sampling was done.

Table 4.2. Moisture Content of Samples from Borehole C3177

Sample Number	Sample Description	Weight Percent Moisture
C3177-45	Composite, Layer 3 Sand	1.78
C3177-80.3	Sediment Associated with Paleosol	5.05
C3177-110	Composite, Layer 2 Sand	2.76
C3177-113.3	Silt lens	5.19
C3177-150	Composite, Layer 2 Sand	2.40
C3177-168.5	Sand, R2	2.24
C3177-170.4	Paleosol	5.26
C3177-200	Composite, Layer 1 Slightly gravelly sand	4.88
C3177-215	Composite, Layer 1 Gravelly sand	2.18
C3177-223.5	Sand, N1	2.22
C3177-242	Sand, R1	2.00
C3177-251	Composite, Layer 1 Sand	1.99

Table 4.3. Moisture Content for Discrete Samples from Borehole C3177[(a)]

Sample Number	Moisture Content (wt. %)	Sample Number	Moisture Content (wt. %)
C3177-5	3.62	C3177 CS-86B	1.78
C3177-10	3.72	C3177 CS-110T	6.29
C3177-15	3.58	C3177 CS-111B	1.80
C3177-20	6.41	C3177 CS-130T	4.73
C3177-25	0.51	C3177 CS-131B	2.44
C3177-30	0.56	C3177 CS-150T	2.33
C3177-35	1.15	C3177 CS-151B	1.88
C3177-40	0.66	C3177 CS-180T	1.68
C3177-45	0.55	C3177 CS-181B	2.53
C3177 CS-45T	1.82	C3177 CS-200T	2.53
C3177 CS-47T	1.86	C3177 CS-201B	2.08
C3177 CS-47B	1.47	C3177 CS-215T	1.51
C3177 CS-49B	2.19	C3177 CS-216B	1.60
C3177 CS-50	1.80	C3177 CS-230T	1.05
C3177 CS-50T	3.07	C3177 CS-231B	1.68
C3177 CS-51B	1.86	C3177 CS-251T	2.07
C3177 CS-60	0.45	C3177 CS-252B	2.55
C3177 CS-65T	2.10	C3177 CS-253T	1.06
C3177 CS-67B	2.29	C3177 CS-255B	2.19
C3177 CS-85T	2.03		

(a) Data supplied by Mr. C. Lindenmeier. Samples not taken from a core sleeve were collected as grab samples in the field. Sample identification numbers are depths below ground surface in feet.
B = Bottom of core sleeve.
CS = Core sample.
T = Top of core sleeve.

The data in Table 4.3 give an indication of the variability of moisture content in samples from the Hanford formation sand-dominated sequence. Given the variable nature of the moisture content, the moisture content of the composite samples taken for this effort is in general agreement with the moisture content of the discrete samples in Table 4.3.

4.3 Bulk Sediment Composition

The bulk composition of each of the twelve samples was measured by XRF. The results are shown in Table 4.4. Iron was reported as FeO by the laboratory. FeO was converted to Fe_2O_3 using the gravimetric conversion factor 1.11134. Iron is reported in Table 4.4 as Fe_2O_3. The totals in Table 4.4 are not normalized and are summed on a volatile free basis. All totals are with about 1.3 wt. % of 100 wt. % except for sample C3177-215.

The weight percent oxides in the samples from borehole C3177 are very similar to those of other samples of the Hanford formation sand-dominated sequence (Serne et al. 2002a) with possible minor exceptions. First, Serne et al. (2002a) report MgO concentrations of 3.0 to 3.8 wt. % for three samples from the Hanford formation sand-dominated sequence although their samples were obtained from 200 West Area boreholes. The MgO concentration of all samples from borehole C3177 is less than 2.6 wt. % and as low as 1.67 wt. %. Second, at borehole 299-E33-338 at the southeast corner of 241-B Tank Farm, the K_2O concentrations in seven samples of Hanford formation sand-dominated sediment were found to be between 1.9 and 2.3 wt. %. This is slightly lower than the K_2O concentrations in Hanford formation Layer 1 and Layer 2 samples from C3177. Finally, the Fe_2O_3 concentrations in the Layer 1 samples from C3177 are slightly higher than the Fe_2O_3 concentrations found in the stratigraphically equivalent samples from borehole 299-E33-338. These differences are probably the result of different laboratories doing the analyses for the different characterization efforts. However, given the relatively few samples involved and the large number of variables that can affect whole sediment chemical composition (e.g., grain-size distribution, degree of weathering, precipitation of secondary phases), the difference is not surprising and is not considered significant with respect to ILAW disposal.

With the exception of the deepest sample from 251 ft bgs, the samples from the Hanford formation Layer 1 appear to have lower SiO_2 and bound water content (from LOI) and greater Fe_2O_3, CaO, and MgO contents than do samples from the Hanford formation Layer 2 and Layer 3. However, the number of samples is small and the number of variables is large, so no general trends can be assumed without a larger database of analyses.

In general, the bulk composition of sediments from borehole C3177 appears to be typical of the Hanford formation sand-dominated sequence.

Table 4.4. Bulk Sediment Composition of Twelve Samples from Borehole C3177

Oxide	C3177-45	C3177-80.3	C3177-110	C3177-113.3	C3177-150	C3177-168.5	C3177-170.4	C3177-200	C3177-215	C3177-223.5	C3177-242	C3177-251
LOI	2.52	2.81	2.32	2.68	2.15	2.07	2.01	2.07	1.76	2.11	1.79	1.95
Major Element Oxides (wt. %)												
SiO_2	71.82	72.19	70.44	72.21	71.45	71.41	72.23	68.43	64.92	67.06	68.44	70.61
Al_2O_3	13.06	13.03	13.24	12.86	13.29	13.23	13.19	13.36	13.65	13.54	13.49	13.53
TiO_2	0.571	0.572	0.672	0.640	0.568	0.545	0.486	0.831	1.118	0.940	0.820	0.603
Fe_2O_3	4.41	4.24	4.91	4.28	4.34	4.39	3.83	6.12	7.68	6.67	5.85	4.66
MnO	0.066	0.069	0.077	0.070	0.072	0.072	0.064	0.098	0.114	0.100	0.091	0.076
CaO	3.31	3.19	3.72	3.44	3.35	3.42	3.22	4.16	5.15	4.52	4.18	3.61
MgO	1.73	1.67	1.87	1.70	1.72	1.71	1.60	2.04	2.62	2.24	2.07	1.72
K_2O	2.63	2.74	2.54	2.36	2.47	2.40	2.44	2.25	2.00	2.16	2.13	2.25
Na_2O	2.73	2.61	2.87	2.71	3.05	3.13	3.20	3.16	3.31	3.25	3.33	3.28
P_2O_5	0.126	0.123	0.153	0.155	0.131	0.128	0.121	0.169	0.219	0.194	0.174	0.138
Trace Elements (μg/g)												
Ni	20	19	20	23	22	26	28	20	19	20	22	24
r	39	43	51	55	53	68	61	55	43	41	47	50
Sc	14	7	11	13	13	15	13	18	27	21	14	17
V	81	62	99	76	81	80	66	120	174	132	131	90
Ba	792	786	810	712	847	865	899	793	767	821	806	842
Rb	87	92	80	77	75	73	72	69	56	66	62	69
Sr	364	362	376	373	404	423	418	404	401	403	414	433
Zr	145	170	145	270	141	145	117	136	140	134	132	123
Y	22	24	22	26	18	19	17	22	28	22	20	18
Nb	10.6	11.7	11.5	13.2	10.5	11.2	9.8	11.0	11.2	10.8	10.1	9.4
Ga	16	15	16	11	17	16	14	16	19	17	13	18
Cu	20	23	22	21	23	23	22	19	27	28	21	18
Zn	49	52	55	53	47	49	49	62	78	67	65	49
Pb	13	13	10	13	9	11	10	8	9	10	12	8
La	29	26	19	29	23	15	23	32	19	36	13	20
Ce	46	51	50	56	49	46	35	46	37	38	40	36
Th	7	5	7	10	6	5	6	6	6	2	3	9
Total (wt. %)	101.333	101.244	101.192	101.195	101.061	100.985	101.001	101.128	103.351	101.044	101.165	100.957

4.4 Carbon Content

The total carbon, inorganic carbon, and organic carbon (by difference) concentrations are shown in Table 4.5 for all twelve samples from borehole C3177. Also shown on the table are the equivalent weight percents of calcium carbonate calculated from the inorganic carbon concentrations. Almost all carbon in the Hanford formation is present as calcium carbonate (calcite).

Table 4.5. Total Carbon, Inorganic Carbon, Equivalent Calcium Carbonate, and Organic Carbon Concentrations in Samples from Borehole C3177

Sample Number	Description	Total Carbon (wt. %)	Mean Total Carbon (wt. %)	Inorganic Carbon (wt. %)	Mean Inorganic Carbon (wt. %)	Equivalent Calcium Carbonate (wt. %)	Organic Carbon[(a)] (wt.%)
C3177-45	Composite, Layer 3 Sand	0.26 0.25	0.25	0.24 0.24 0.24	0.24	1.99	0.01
C3177-80.3	Sediment Associated with Paleosol	0.22		0.22		1.83	0.00
C3177-110	Composite, Layer 2 Sand	0.20		0.19		1.58	0.01
C3177-113.3	Silt lens	0.23		0.21		1.75	0.02
C3177-150	Composite, Layer 2 Sand	0.20		0.17		1.42	0.03
C3177-168.5	Sand, R2	0.21		0.15		1.25	0.06
C3177-170.4	Paleosol	0.20		0.17		1.42	0.03
C3177-200	Composite, Layer 1 slightly gravelly sand	0.18		0.14 0.15	0.14	1.16 1.25	0.04
C3177-215	Composite, Layer 1 gravelly sand	0.11		0.7		0.58	0.04
C3177-223.5	Sand, N1	0.14		0.10		0.83	0.04
C3177-242	Sand, R1	0.19 0.22	0.21	0.16		1.33	0.05
C3177-251	Composite, Layer 1 sand	0.17		0.13		1.08	0.04
(a) Organic carbon calculated by difference.							

All the total carbon, inorganic carbon, and organic carbon values obtained from borehole C3177 samples are within the reported range of sediments from the Hanford formation sand-dominated sequence (Serne et al. 2002a) but are on the low end of the range. However, all values are reasonable considering that (1) the samples collected by Serne et al. (2002a) and used here for comparison, were from areas of the Hanford Site other than the ILAW site and (2) the amount of calcium carbonate in the sediments is a function of the length of time available for soil development and the amount of detrital calcium carbonate deposited by the cataclysmic floods in a given area.

As expected, the coarser grained sediments, with significant gravel components, contain less weight percent calcium carbonate than finer grained sediments (with the exception of the sample from 251 ft depth). Somewhat surprising, however, is the relatively low calcium carbonate content of the paleosols. The paleosols present in borehole C3177 did not develop over the relatively long periods of time or in the same weathering environment available for development of other, more developed, paleosols such as those found as part of the Cold Creek unit that commonly contains up to 4.5 to 5 wt % carbon (or approximately 38 wt. % calcium carbonate). Instead, the paleosols in the Hanford formation at borehole C3177 probably developed in only a few thousand years between flood deposits. The paleosols at borehole C3177 were recognized by their mud content, bioturbated, and bleached nature (Reidel et al. 2001) and not as a well-developed caliche.

4.5 Mineralogy

XRD analysis of the ILAW borehole C3177 sediments shows that all the samples are mineralogically similar. The bulk sediments are dominated by quartz and feldspar (both plagioclase and alkali-feldspar), with lesser amounts of mica, chlorite, and an amphibole.

Semi-quantitative analyses of the minerals in the bulk samples are provided in Table 4.6. Quartz concentrations range from 26 wt. % to 46 wt. %, with an average quartz concentration of 38 ± 6 wt. %. Plagioclase feldspar is present at concentrations between 15 to 40 wt. % and potassium feldspar concentrations are between 16 to 31 wt. %. Plagioclase feldspar was more abundant than potassium feldspar in all samples except C3177-45, C3177-80.3, C3177-113.3, and C3177-170.4. Overall, the feldspar content (both plagioclase and alkali feldspars) averaged about 47 ± 5 wt. %. The amphibole phase comprised <4 wt. %, with the majority of samples having concentrations in the 2 to 4 wt. % range.

Samples from Hanford formation Layer 1 have higher plagioclase and lower quartz concentrations than do samples from Layer 2 or Layer 3. This reflects to the greater basalt content in Layer 1 than in the overlying layers (see the physical descriptions of samples in Table 2.2). Also, the paleosols and the silt lens have greater potassium feldspar concentrations than do the other samples.

Calcite was identified in the physical description of most of the sediments by effervescence with HCl. However, calcite was not identified in any of the sediments by XRD. This suggests that calcite makes up less than a few percent of the samples, and that the major calcite reflections were masked by reflections from more abundant minerals in the diffraction analyses. The conversion of inorganic carbon to equivalent amounts of calcite also indicates that calcite is a minor phase (Table 4.5).

Table 4.6. Semi-Quantitative X-ray Diffraction Results of Bulk Samples from Borehole C3177

Sample Number	Mineral Phase (wt-%)						Goodness of fit[(a)]
	Quartz	Amphibole	Plagioclase	K-Spar	Mica	Chlorite	
C3177-45	43	2	20	20	11	3	0.87
C3177-80.3	41	2	15	28	16	2	0.94
C3177-110	46	1	25	19	9	2	0.70
C3177-113.3	40	4	15	31	8	2	1.22
C3177-150	42	3	25	18	3	8	0.81
C3177-168.5	40	4	23	22	10	2	1.00
C3177-170.4	43	3	21	23	8	2	1.04
C3177-200	37	4	31	16	10	3	0.77
C3177-215	26	3	40	18	11	3	0.73
C3177-223.5	33	4	34	18	8	3	0.56
C3177-242	32	2	31	18	14	3	0.95
C3177-251	32	4	35	18	9	3	0.67
(a) Values closest to 1.0 represent an ideal refinement.							

Clay minerals identified in the bulk sediments include mica and chlorite. Mica concentrations range from 3 wt. % to 16 wt. % (the paleosol at 80.3 ft bgs), with an average concentration of 10 ± 3 wt. %. The specific type of mica present in the samples was not determined by XRD, but both muscovite and biotite were identified during physical descriptions of the samples. Chlorite concentrations were <3 wt. % in all sediments analyzed with the exception of sample C3177-150, which had 8 wt. % chlorite.

The results of XRD analysis of the <1.4 μm fraction of each sample are shown in Table 4.7. The clay fractions are dominated by four clay minerals: smectite, chlorite, illite, and kaolinite with minor amounts of quartz and feldspar. Figure 4.7 provides an example XRD pattern of a typical clay assemblage (sample C3177-80.4).

No general trends are noted in the data in Table 4.7 from the twelve ILAW samples. Smectite concentration ranges from 18 wt. % to 39 wt. %. Illite concentration varies from 43 to 54 wt. % with an average concentration of 48 wt. %. Chlorite and kaolinite are the least abundant of the clay minerals identified in the samples with concentrations equal to or less than 24 wt. % and 9 wt. %, respectively. Quartz and feldspar minerals were present as trace amounts in the clay fraction and therefore were not included in totals presented in Table 4.7.

The silt lens sample (C3177-113.3) has the highest smectite concentration, and the lower paleosol sample (C3177-170.4) has the highest chlorite concentration. Overall, the mineralogy of the clay fractions from borehole C3177 is similar to clay fractions analyzed from clean boreholes and other composite samples of the Hanford formation sand-dominated sequence characterized by Serne et al. (2002a).

Table 4.7. Semi-Quantitative X-ray Diffraction Results of Clay Minerals Separated from the Samples Collected from Borehole C3177

Sample Number	Mineral Phase (wt. %)				Normalization Factor
	Smectite	Illite	Chlorite	Kaolinite	
C3177-45	24	54	14	8	0.67
C3177-80.3	34	44	14	9	0.78
C3177-110	26	51	16	7	0.89
C3177-113.3	39	43	12	6	0.90
C3177-150	25	50	18	7	0.77
C3177-168.5	27	47	19	6	0.90
C3177-170.4	18	50	24	9	1.40
C3177-200	27	50	16	8	1.36
C3177-215	30	46	20	4	1.50
C3177-223.5	NA	NA	NA	NA	-
C3177-242	27	44	18	10	1.16
C3177-251	NA	NA	NA	NA	-
NA = not analyzed.					

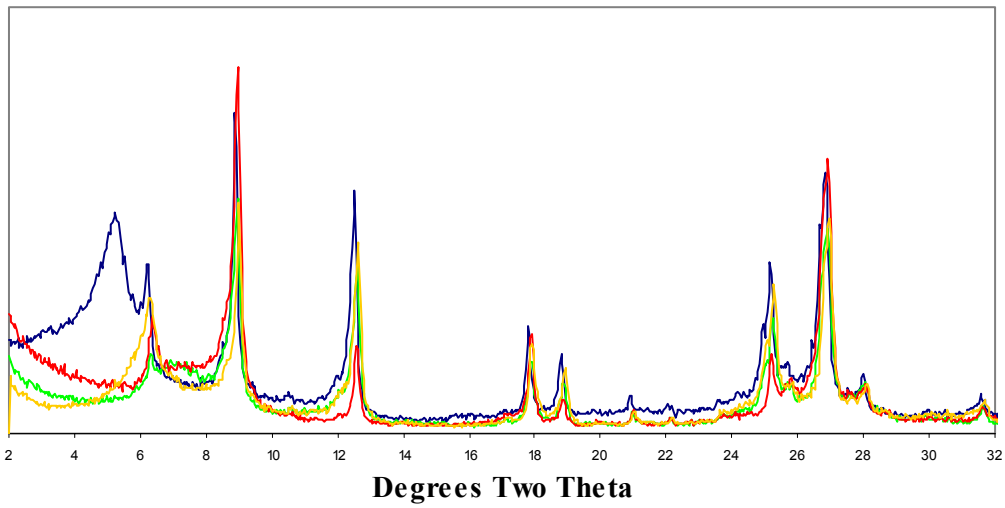

Figure 4.7. X-ray Diffraction Tracings of Preferentially Oriented <1.4 μm Specimen from Sample C3177-80.3. The scans were collected from 2 to 45° 2θ with a 0.04° step and 2-second dwell time. The yellow line represents the Mg-saturated fraction and the blue line represents the same fraction solvated with ethylene glycol. The green line indicates the K^+ saturation and the red line is the K^+-saturated sample heated to 575°C for 1 hour.

Total clay recoveries are within ±15% of the "ideal" 100% for samples C3177-110, C3177-113.3, C3177-168.5, and C3177-242.0. Most other samples have recoveries within 30% of the "ideal" 100%. Factors affecting the semi-quantification procedure (preparation and condition of the clay filter cake) were generally controlled and not thought to be significant. Quantitative analysis is considered good if errors amount to ±10% of the amounts present for major constituents and ±20% for minerals whose concentrations are less than 20% (Moore and Reynolds 1989).

In 2000, the mineralogy of eight representative core samples from ILAW borehole 299-E17-21 was determined by XRD. The report prepared in 2000 containing the results of the 2000 characterization effort is included as Appendix B to this report. (Note: Some the formulas for anorthorite, chamosite, muscovite and illite listed in the tables of the 2000 report in Appendix B have been changed because they were in error in the original report.) The report in Appendix B cites the specific mineral species anorthite, orthoclase, muscovite, chamosite, and ferrotschermakite. Those results should be reported as plagioclase feldspar, potassium feldspar, mica, chlorite and amphibole respectively. This is because the analyses done for the 2000 characterization were not detailed enough to indicate specific species. Knowledge of the specific species of feldspars, amphiboles, chlorites, and micas present in the sediments is probably not necessary to predict the performance of the ILAW disposal site.

4.6 Surface Area

The surface area of the bulk sediment (with particles > 7mm excluded) and the clay-size fraction (<1.4 μm) was measured for each of the composite samples. Several other sediment sample clay-size fractions were also measured and the data are given in Table 4.8. The data represent the external surface area per gram of sample that is available to react with non-polar molecules. (Note: In this case, N_2 was used for the measurement. N_2 does not readily penetrate the interlayers of the clay minerals so that only the external surfaces contribute to the measurement.) There are no available previously measured values of surface area for the Hanford formation H2 sand-dominated sequence for comparison. The surface area values for the bulk sediments are similar to a value recently found for a near-surface Hanford formation sand-dominated sequence in the 300 Area (Serne et al. 2002b). The 300 Area sand-dominated sediment had a BET surface area value of 5.6 ± 0.4 m^2/g.

The surface area of the bulk sediments from the ILAW borehole are low and quite similar except the composite sample from 215 ft bgs, which contains both a high percentage of coarse pebbles and fine sand/silt. It was hard to get similar small aliquots (~2 g) of this sediment that excluded the coarse pebbles, which would not fit into the surface area analyzer but would represent the finer fraction. Three aliquots were run that yielded individual values of 15.58, 7.51, and 7.92 m^2/g. The average value and standard deviation are reported in Table 4.8. This sample appears to have a higher surface area than the other bulk sediments from the borehole. As shown in Table 4.6, this sample appears to contain less quartz and more plagioclase than any of the other composites that were created. Perhaps the lower quartz content leads to higher bulk surface area.

The values for the clay-size fractions in Table 4.8 appear to be reasonable if they are compared to the mineralogy of the samples and to published values for monomineralic clay samples. Grim (1968) reports the following range of values for BET determined surface area: smectite 30 to 82 m^2/g, illite 56 to 113 m^2/g, and kaolinite 16 to 22 m^2/g. No values are given for chlorite. In addition, the clay-size fraction for the 300 Area sediment had a BET surface area of 62.8 ± 1.2 m^2/g (Serne et al. 2002b). The composite sample clay fraction surface areas do not show any unique differences and all values are 10 to 30% lower than for the clay-size fraction in the one near surface sediment from the 300 Area sample.

Table 4.8. Surface Area of Twelve Clay-Size Fractions from Borehole C3177

Sample Number	Bulk Sediment (m2/g)	Clay-Size (m^2/g)
C3177-45	3.936	51.1
C3177-80.3		53.0
C3177-110	5.112	41.8
C3177-113.3		21.1
C3177 150	3.517	38.4
C3177-168.5		28.3
C3177-170.4		35.1
C3177-170.4 rerun		35.0
C3177-200	5.296	52.5
C3177-215	7.51	52.2
C3177-215 rerun	10.3 ± 4.5[(a)]	
C3177-223.5		58.5
C3177-242		36.9
C3177-251	4.43	46.8

(a) Sample has high percentage of pebbles that cannot fit into instrument and high percentage of fine sand/silt. Therefore, three aliquots (with pebbles selectively excluded) were run. A more precise value could be obtained by removing all particles larter than the size that would fit in the analyzer and homogenizing the finer fraction.

4.7 1:1 Water Extracts

4.7.1 pH, Electrical Conductivity, and Alkalinity

Table 4.9 gives the pH, alkalinity, and electrical conductivity for 1:1 water to sediment extracts of the twelve samples from borehole C3177. The electrical conductivity is given as both the electrical conductivity of the 1:1 water extract and as dilution corrected electrical conductivity. Electrical conductivity as 1:1 water extract is easily related to electrical conductivity per gram of soil. The dilution-corrected

electrical conductivity easily related to the electrical conductivity of the actual pore water if one assumes that the addition of distilled water did not dissolve any solid material and was, thus, only a diluent.

The alkalinity, pH, and electrical conductivity of the twelve samples in Table 4.9 are within the range of these parameters measured on other uncontaminated samples of the Hanford formation sediments (Serne et al. 2002a). The most notable sample is the sample associated with the upper paleosol at approximately 80 ft bgs. This sample has a very high 1:1 water extract electrical conductivity. This electrical conductivity is associated with high calcium, chloride, nitrate, and sulfate in the sample.

Table 4.9. Alkalinity, pH, and Electrical Conductivity of Samples from Borehole C3177

Sample Number	Description	Alkalinity (mg $CaCO_3$/L)	pH	1:1 Water Extract Electrical Conductivity (μS/cm)	Dilution Corrected Electrical Conductivity (μS/cm)
C3177-45	Composite, Layer 3 sand	42.9	7.31	204	11,459
C3177-80.3	Sediment Associated with Paleosol		7.35	375	7,493
C3177-110	Composite, Layer 2 sand	39.78	7.41	141	5,121
C3177-113.3	Silt lens		7.42	196	3,784
C3177-150	Composite, Layer 2 Sand	45.24	7.54	131	5,444
C3177-168.5	Sand, R2		7.45	123	5,516
C3177-170.4	Paleosol		7.46	179	3,404
C3177-200	Composite, Layer 1 Slightly gravelly sand	40.56	7.60	164	3,371
C3177-215	Composite, Layer 1 Gravelly sand	43.68	7.54	199	9,142
C3177-223.5	Sand, N1		7.66	184	8,305
C3177-242	Sand, R1		8.38	112	5,601
C3177-251	Composite, Layer 1 sand	40.56	7.57	201	10,079

Also of note are the samples from 223.5 and 242 ft bgs, taken above and below the N1/R1 paleomagnetic boundary. These two samples have the highest pH values measured from the twelve samples with the 242-ft-deep sample (below the boundary) having the highest pH. There is also a distinct electrical conductivity difference between these two samples. The sample above the N1/R1 contact has higher electrical conductivity, associated with higher calcium, chloride, nitrate, and sulfate, than does the sample below the contact.

The composite samples from Hanford formation Layer 2 (C3177-110 and C3177-150) have lower electrical conductive values than the composite samples from the overlying Layer 3 (C3177-45) and the underlying Layer 1 (C3177-251). Also, the silt sample, from within Layer 2 (C3177-113.3), has an electrical conductivity greater than that of the overlying and underlying Layer 2 composite samples. Generalizations about differences among the sedimentary layers will require more than the six available analyses in Table 4.9.

For comparison, Table 4.10 shows the results of pH and electrical conductivity in samples from borehole C3177 that were obtained for purposes of recharge studies. The data show the variability in pH and electrical conductivity in discrete samples from the Hanford formation in the area of the ILAW site. The data also show that the 1:1 water extracts from samples of Hanford formation Layer 2 (Layer 2 extends from 78 to 170 ft bgs) and the upper part of Layer 1 (Layer 1 extends from 170 to 270 ft bgs) have lower electrical conductive values than do samples from Layer 3 (Layer 3 extends from the surface to 78 ft bgs) and the lower part of Layer 1. This "trend" in electrical conductivity shown by the discrete samples in Table 4.10 agrees with the data from the composite samples in Table 4.9 where the electrical conductivity of the composite Layer 2 samples is less than that of the overlying Layer 3 sample and the underlying Layer 1 samples.

Table 4.10. Electrical Conductivity and pH for Discrete Samples from Borehole C3177[(a)]

Sample Number	pH	1:1 Water Extract Electrical Conductivity (μS/cm)	Sample Number	pH	1:1 Water Extract Electrical Conductivity (μS/cm)
C3177-5	7.40	176	C3177 CS-86B	7.93	143
C3177-10	8.30	345	C3177 CS-110T	7.71	246
C3177-15	8.20	304	C3177 CS-111B	7.51	201
C3177-20	7.82	449	C3177 CS-130T	7.72	ND
C3177-25	7.50	161	C3177 CS-131B	7.82	ND
C3177-30	7.51	196	C3177 CS-150T	7.74	144
C3177-35	7.42	187	C3177 CS-151B	7.82	137
C3177-40	7.31	231	C3177 CS-180T	7.66	131
C3177-45	7.38	213	C3177 CS-181B	7.72	137
C3177 CS-45T	7.42	211	C3177 CS-200T	7.89	165
C3177 CS-47T	7.43	244	C3177 CS-201B	7.88	140
C3177 CS-47B	7.47	183	C3177 CS-215T	7.67	216
C3177 CS-49B	7.48	202	C3177 CS-216B	7.42	231
C3177 CS-50	7.36	222	C3177 CS-230T	7.60	202
C3177 CS-50T	7.45	244	C3177 CS-231B	7.55	184
C3177 CS-51B	7.73	207	C3177 CS-251T	7.57	ND

Table 4.10. (Cont.)

C3177 CS-60	7.37	201	C3177 CS-252B	7.54	169
C3177 CS-65T	7.91	180	C3177 CS-253T	7.43	244
C3177 CS-67B	7.84	186	C3177 CS-255B	7.66	171
C3177 CS-85T	7.97	144			

(a) Data supplied by Mr. C. Lindenmeier. Samples not taken from a core sleeve were collected as grab samples in the field. Sample identification numbers are depths below ground surface in feet.
B = Bottom of core sleeve.
CS = Core sample.
ND = Not determined.
T = Top of core sleeve

4.7.2 1:1 Water Extract Metals

The concentrations of selected metals in 1:1 water extracts are shown in Table 4.11. All results from analyses of 30 major and trace metals are given in the Appendix A. The data show that calcium and sodium are the major cations on a mass basis, and that calcium and magnesium are the major cations on a milliequivalent basis in the water extracts. This was also the case for water extract analyses of samples from the Hanford formation sand-dominated sequence in two clean boreholes studied by Serne et al. (2002a) and for seven samples from borehole 299-E33-338. The sodium concentrations from borehole C3177 are generally higher than sodium concentrations in samples from borehole 299-E33-338, which ranged from about 4,400 to 17,500 μg/L. The cation concentrations measured in samples from borehole C3177 are generally lower than the range, or on the low end of the range, of cation concentrations measured from the two clean boreholes from 200 West Area and described by Serne et al. (2002a).

The water extract associated with the sample at 80.3 ft bgs has the highest dissolved solids of all the samples. Also, the water extracts from the composite samples from Hanford formation Layer 2 have lower potassium, magnesium, sodium and sulfur than do the extracts from Layer 1 and Layer 3 samples. However, the data set is very limited and such generalizations are tentative.

Table 4.11. Concentrations of Major Metals in 1:1 Water Extracts[(a)]

Sample Number	Description	Al (µg/L)	Ca (µg/L)	Fe (µg/L)	K (µg/L)	Mg (µg/L)	Na (µg/L)	S (µg/L)	Si (µg/L)
C3177-45	Composite, Layer 3 sand	41	7,825	30	5,356	3,370	19,032	11,547	9,384
C3177-80.3	Sediment Associated with Paleosol	ND	27,766	16	7,481	11,539	20,101	28,780	10,179
C3177-110	Composite, Layer 2 sand	45	5,795	41	3,716	1,880	15,841	4,385	10,059
C3177-113.3	Silt lens	(9)	13,207	11	3,758	4,003	13,739	8,854	7,884
C3177-150	Composite, Layer 2 sand	39	7,548	27	3,390	2,305	10,264	3,740	7,469
C3177-168.5	Sand, R2	37	6,943	29	2,941	2,008	11,470	3,991	7,023
C3177-170.4	Paleosol	60	8,745	25	5,216	2,684	19,429	5,055	7,658
C3177-200	Composite, Layer 2 slightly gravelly sand	34	8,663	21	4,551	2,963	14,926	9,537	10,328
C3177-215	Composite, Layer 2 gravelly sand	43	11,995	20	5,341	3,985	15,349	17,154	9,748
C3177-223.5	Sand, N1	(22)	10,702	15	4,775	3,665	15,105	13,975	9,892
C3177-242	Sand, R1	56	2,809	52	2,862	927	18,810	1,600	11,150
C3177-251	Composite, L1 sand	50	13,528	25	4,511	4,072	13,436	15,968	8,460

(a) Values in parentheses are less than limit of quantitation.
ND = Not determined.

Table 4.12 shows major cation concentrations in 1:1 water extracts in several discrete samples from borehole C3177. The data in Table 4.12 were obtained for other purposes (recharge studies). As with the data in Table 4.11, the cation concentrations in Table 4.12 show that the concentrations of magnesium, potassium, and sulfur tend to be lower and iron tends to be higher in Hanford formation Layer 2 and the top of Layer 1 (between about 85 and 201 ft bgs) than in Layer 3 and lower Layer 1, but several exceptions exist.

In summary, there does not appear to be any unusual features in the cations concentrations of samples from borehole C3177.

Table 4.12. Major Cations in 1:1 Water Extracts from C3177 Core and Grab Samples[(a)]

Sample Number	Al (μg/mL)	Ca (μg/mL)	Fe (μg/mL)	K (μg/mL)	Mg (μg/mL)	Na (μg/mL)	S (μg/mL)	Si (μg/mL)
C3177-5	(0.035)	13.148	0.040	(1.460)	2.705	14.149	4.768	16.964
C3177-10	0.304	4.302	0.192	(1.722)	1.051	71.706	19.555	13.678
C3177-15	0.232	3.641	0.113	(1.498)	1.014	64.248	12.394	11.588
C3177-20	0.123	4.946	0.049	(1.948)	1.258	90.988	29.209	9.926
C3177-25	0.125	6.779	0.087	3.469	2.962	15.806	4.959	8.782
C3177-30	0.080	7.372	0.234	4.196	3.191	21.615	8.012	9.342
C3177-35	0.086	7.779	0.061	4.617	3.387	21.741	7.798	9.008
C3177-40	0.052	10.717	0.066	5.360	4.850	20.509	14.352	8.896
C3177-45	(0.021)	12.243	(0.007)	5.379	5.338	15.710	13.681	9.826
C3177 CS-45T	0.077	7.145	0.813	4.673	3.006	25.434	12.992	8.411
C3177 CS-47T	0.137	11.248	0.107	5.953	5.031	11.519	9.989	8.332
C3177 CS-47B	0.063	15.855	0.167	6.952	7.166	13.743	16.024	7.598
C3177 CS-49B	(0.034)	12.985	(0.014)	5.582	5.500	13.450	11.969	10.131
C3177 CS-50	(0.019)	12.882	(0.013)	6.069	5.251	15.362	16.573	8.094
C3177 CS-50T	(0.013)	13.837	(0.002)	5.918	5.972	19.116	18.454	9.471
C3177 CS-51B	(0.045)	12.994	0.081	6.585	5.211	13.575	12.903	9.262
C3177 CS-60	0.064	10.189	0.030	5.049	4.299	16.851	13.179	8.671
C3177_CS-65T	0.091	9.250	0.066	5.985	3.905	15.308	10.015	8.664
C3177 CS-67B	0.137	9.767	0.830	7.158	4.108	15.158	9.565	9.049
C3177 CS-85T	0.116	7.275	0.102	5.065	2.837	12.888	4.461	9.432
C3177 CS-86B	0.115	7.698	0.074	5.210	3.022	11.709	3.971	9.050
C3177 CS-110T	0.063	13.252	0.044	5.376	3.962	25.756	13.994	8.291
C3177 CS-111B	(0.027)	14.587	0.126	4.430	4.502	13.824	11.296	8.613
C3177 CS-130T	0.059	11.873	0.029	5.752	3.528	17.403	7.993	8.721

Table 4.12. (Cont.)

Sample Number	Al (μg/mL)	Ca (μg/mL)	Fe (μg/mL)	K (μg/mL)	Mg (μg/mL)	Na (μg/mL)	S (μg/mL)	Si (μg/mL)
C3177 CS-131B	0.121	8.921	0.092	4.229	2.610	11.385	4.665	9.473
C3177 CS-150T	0.087	8.762	0.049	4.396	2.829	11.972	4.285	8.824
C3177 CS-151B	0.085	8.410	0.065	4.198	2.687	10.854	4.150	8.907
C3177 CS-180T	0.161	7.442	0.176	4.689	2.493	12.497	4.258	10.121
C3177 CS-181B	0.197	7.159	0.500	4.891	2.475	12.118	4.122	10.822
C3177 CS-200T	0.179	7.748	0.202	4.909	2.532	16.611	8.735	8.953
C3177 CS-201B	0.220	6.986	0.217	4.808	2.367	12.687	6.201	9.533
C3177 CS-215T	0.058	13.547	0.136	6.123	4.719	17.106	18.399	8.105
C3177 CS-216B	0.050	16.330	0.037	6.409	5.719	15.868	21.575	8.539
C3177 CS-230T	0.082	12.766	0.072	6.354	4.326	16.429	14.015	8.345
C3177 CS-231B	0.109	11.475	0.104	6.006	3.988	14.841	13.965	8.076
C3177 CS-251T	0.102	9.586	0.108	4.858	3.175	11.840	10.544	8.099
C3177 CS-252B	0.071	9.763	0.064	5.432	3.239	13.651	10.655	8.696
C3177 CS-253T	(0.021)	18.261	(0.018)	6.037	6.027	15.176	23.933	7.853
C3177 CS-255B	0.089	10.499	0.485	5.019	3.407	12.695	11.685	7.912

(a) Data supplied by Mr. C. Lindenmeier. Samples not taken from a core sleeve were collected as grab samples in the field. Sample identification numbers are depths below ground surface. Values in parentheses are less than limit of quantitation.
CS = Core sample.
T = Top of core sleeve.
B = Bottom of core sleeve.

4.7.3 1:1 Water Extract Anions

Analytical results for measurements of anion concentrations are shown in Tables 4.13 and 4.14. The limited number of data suggests that, with the exception of paleosols and silt lens, nitrate and sulfate concentrations are relatively low and chloride concentration is relatively high in Hanford formation Layer 2 as compared with Layers 1 and 3. The upper paleosol, at 80.3 ft bgs, and to a lesser extent the silt lens at 113.3 ft bgs, are relatively high in nitrate chloride and sulfate. The lower paleosol does not share this characteristic. Also, there is a large difference in anion concentrations across the N1/R1 boundary between 223.5 and 242.0 feet bgs.

Table 4.13. Anion Concentrations in Samples from Borehole C3177 (mg/g of soil)

Sample Number	Nitrate	Chloride	Sulfate	Phosphate	Fluoride
C3177-45	2.66	4.16	31.26	0.24	0.22
C3177-80.3	6.50	32.63	74.75	0.24	0.51
C3177-110	0.35	3.03	11.73	0.24	0.34
C3177-113.3	6.52	8.65	29.76	0.24	0.50
C3177-150	0.48	3.50	9.79	0.24	0.31
C3177-168.5	0.48	1.30	9.96	0.24	0.31
C3177-170.4	0.55	10.40	16.03	0.24	0.52
C3177-200	0.48	2.60	24.83	0.24	0.37
C3177-215	1.34	1.38	56.53	0.24	0.41
C3177-223.5	1.84	1.76	46.59	0.24	0.35
C3177-242	0.38	0.06	8.57	0.81	0.04
C3177-251	4.96	1.34	53.17	0.24	0.31

Table 4.14. Anion Concentrations in Samples from Borehole C3177 (μg/ml of pore water)

Sample Number	Nitrate	Chloride	Sulfate	Phosphate	Fluoride
C3177-45	149.19	233.74	1,754.90	13.48	12.58
C3177-80.3	128.76	646.50	1,480.89	4.80	10.08
C3177-110	12.87	109.93	425.81	8.72	12.30
C3177-113.3	125.65	166.76	573.55	4.63	9.55
C3177-150	19.89	145.78	407.27	9.97	12.95
C3177-168.5	21.52	58.30	445.30	10.76	13.90
C3177-170.4	10.44	197.77	304.82	4.56	9.89
C3177-200	9.78	53.23	509.18	4.93	7.51
C3177-215	61.53	63.55	2,594.81	11.03	18.60
C3177-223.5	82.59	79.41	2,096.41	10.83	15.97
C3177-242	19.00	3.00	428.54	40.50	2.00
C3177-251	248.62	67.27	2,666.60	12.03	15.58

Table 4.15 shows anion concentrations from several discrete samples from borehole C3177. The data in Table 4.15 were obtained for purposes of recharge studies and not as part of this characterization. As with the data in Tables 4.13 and 4.14, the anion concentrations in Table 4.15 show that Hanford formation Layer 2 (between 78 and 170 ft bgs) is relative low in nitrate and sulfate as compared with Layer 1 (170 to 270 ft bgs) and Layer 3 (surface to 78 ft bgs). The chloride concentrations in Table 4.15 for Layer 2 samples appear to be low as compared with the chloride concentrations in samples from Layer 1 and

Layer 3. This is the opposite of chloride "trend" seen in Table 4.13, although the small number of data makes that observation tentative. Overall, the anions concentrations obtained for this characterization effort (Tables 4.13 and 4.14 are at the low end of the ranges of anion concentrations shown on Table 4.15.

Table 4.15. Anion Concentrations in 1:1 Water Extracts from C3177 Core and Grab Samples (μg/ml of pore water) [(a)]

Sample Number	Fluoride	Chloride	Bromide	Nitrate	Phosphate	Sulfate
C3177-5	23.77	95.06	MDL	189.54	11.59	362.43
C3177-10	33.11	160.34	0.29	63.90	19.17	1,737.03
C3177-15	24.17	199.93	0.30	57.59	15.22	1,077.23
C3177-20	11.74	399.67	0.88	61.35	5.43	1,586.42
C3177-25	79.31	1,155.94	3.97	765.34	35.69	2,637.04
C3177-30	75.54	1,996.37	7.19	767.97	35.97	4,136.63
C3177-35	29.44	1,150.93	3.57	24.98	12.49	1,971.76
C3177-40	58.35	1,934.89	7.68	548.22	24.57	6,741.39
C3177-45	70.25	571.24	1.85	861.49	27.73	7,764.46
C3177 CS-45T	17.71	203.99	0.57	117.14	4.57	2,285.60
C3177 CS-47T	20.93	160.65	1.13	87.11	3.96	2,862.30
C3177 CS-47B	18.86	115.24	0.70	208.84	2.79	2,039.47
C3177 CS-49B	14.38	80.04	MDL	85.79	5.27	1,653.42
C3177 CS-50	22.58	143.01	1.16	289.49	5.21	2,854.41
C3177 CS-50T	9.23	131.02	0.71	74.92	1.42	1,931.58
C3177 CS-51B	16.27	95.40	0.56	107.18	MDL	2,070.73
C3177 CS-60	67.93	733.61	4.53	962.30	36.23	8,739.97
C3177_CS-65T	13.40	85.85	0.99	MDL	2.48	1,374.52
C3177 CS-67B	17.35	64.83	0.46	70.77	7.30	1,209.87
C3177 CS-85T	13.79	63.33	MDL	MDL	3.57	566.86
C3177 CS-86B	17.68	67.78	0.59	MDL	8.84	558.11
C3177 CS-110T	5.88	110.03	0.36	54.48	MDL	745.97
C3177 CS-111B	14.87	286.12	1.19	76.74	MDL	1,945.17
C3177 CS-130T	10.42	47.22	0.23	MDL	2.78	500.00
C3177 CS-131B	13.30	46.77	MDL	MDL	8.15	493.41

Table 4.15. (Cont)

Sample Number	Fluoride	Chloride	Bromide	Nitrate	Phosphate	Sulfate
C3177 CS-150T	15.29	33.74	MDL	MDL	4.50	476.82
C3177 CS-151B	16.08	44.91	MDL	MDL	8.87	565.54
C3177 CS-180T	19.54	32.14	MDL	MDL	11.34	642.82
C3177 CS-181B	12.48	16.64	0.42	0.42	7.49	415.27
C3177 CS-200T	14.94	50.21	0.41	1.66	4.56	1,029.07
C3177 CS-201B	13.50	23.99	MDL	MDL	8.50	824.80
C3177 CS-215T	19.72	101.29	MDL	MDL	6.80	3,664.28
C3177 CS-216B	15.54	105.57	MDL	3.89	7.12	3,931.39
C3177 CS-230T	25.35	128.72	MDL	MDL	8.78	3,803.03
C3177 CS-231B	13.71	85.40	MDL	MDL	5.61	2,375.08
C3177 CS-251T	10.56	28.66	MDL	112.63	7.04	1,448.10
C3177 CS-252B	12.70	27.94	MDL	41.91	3.81	1,231.93
C3177 CS-253T	25.27	144.80	0.97	257.52	4.86	6,462.41
C3177 CS-255B	11.49	38.78	0.48	154.63	7.18	1,527.16

(a) Data supplied by Mr. C. Lindenmeier. Samples not taken from a core sleeve were collected as grab samples in the field. Sample identification numbers are depths below ground surface.
B = Bottom of core sleeve.
CS = Core sample.
MDL = Indicates that concentration was less than minimum detection limit.
T = Top of core sleeve.

4.8 Iron Extractions

Results from the iron extraction experiments are presented in Figure 4.8. Similar to previously published results (Tessier et al. 1979; McAlister and Smith 1999), the sodium dithionite containing solutions removed more iron from the composite soil samples than the less aggressive extraction solutions. Overall, the total percentages of iron extracted from the various samples are lower than those reported from similar tests performed on an exposed Hanford Site soil collected in the vicinity of the 300 Area (Serne et al. 2002b). The relatively low extractable iron concentrations in the ILAW samples may be attributed to short times that the samples were exposed to the weathering environment. The samples are sands that were rapidly deposited from glacial floods and probably were not exposed to the weathering environment for any appreciable time before being buried by overlying sediment. This conceptual model is further supported by the extraction data, which indicate that iron oxide precipitates and coatings constitute less than 0.3 wt. % in all of the composite samples. These data suggest that iron

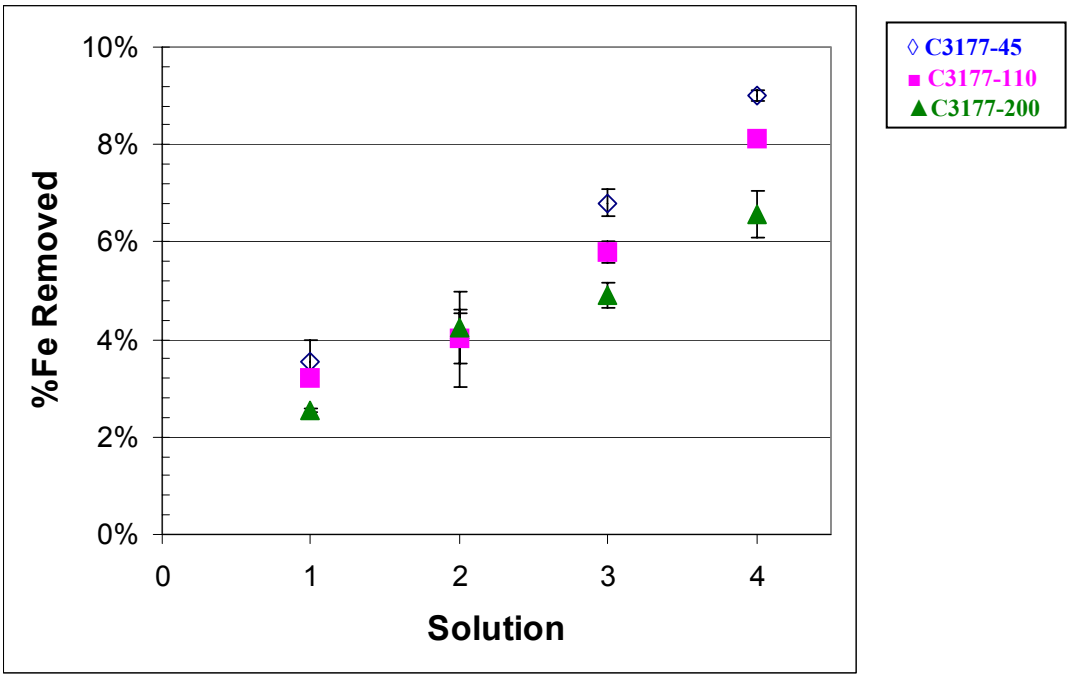

Figure 4.8. Percentage of Iron Removed from Borehole C3177 Composite Samples. (The solution numbers on the x axis correspond to the following solutions: 1–Hydroxylamine Hydrochloride/Acetic Acid, 2–Ammonium Oxalate/Oxalic Acid, 3–Sodium Dithionite/Sodium Citrate/Sodium Bicarbonate, and 4–Sodium Dithionite/Sodium Citrate/Citric Acid.)

oxide measurements taken from exposed faces and outcroppings can potentially overestimate the percentages available in buried Hanford formation flood deposits. It is difficult to discern from the data the overall effectiveness of the respective solutions to target discrete iron phases (i.e. amorphous versus crystalline). Characterization and comparison of the leached versus non-leached sediment by techniques such as scanning electron microscopy and x-ray diffraction would need to be utilized to further evaluate whether the classical extraction techniques can differentiate amorphous from crystalline ferric oxides in Hanford formation sands, which are relatively young and unweathered.

4.9 Cation Exchange Capacities

Figure 4.9 is a graph of the total calculated CEC of three composite samples from borehole C3177 using three separate radio-tracer techniques. For comparison, some of the samples were pretreated with a slightly acidic sodium acetate solution to remove any discrete carbonate solids and carbonate coatings that might be present in the sediments. In general, agreement between the three techniques is quite good (average relative standard deviation of 11%), with the largest portion of error assigned to the ^{22}Na replicate analysis for sample C3177-45. Slightly better agreement was achieved using the Cs^{137} and ^{85}Sr tracers; therefore, future analyses will utilize the ^{85}Sr radio-tracer method. An interesting result to note is that the relative standard deviation is actually lower (less than 11%) when the calculation is performed

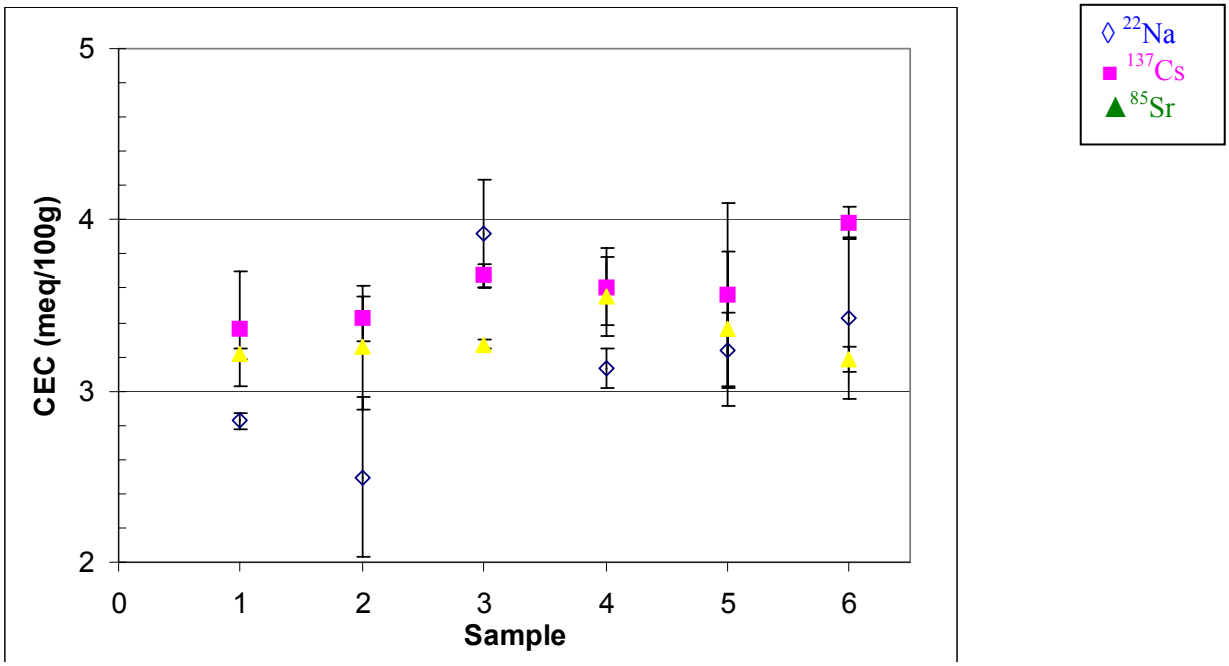

Figure 4.9. Calculated Cation Exchange Capacities of Composite Samples from Borehole C3177. (The sample numbers on the x–axis correspond to: 1–C3177-45 NaOAc treated, 2–C3177-45 non-treated, 3–C3177-110 NaOAc treated, 4–C3177-110 non-treated, 5-C3177-200 NaOAc treated, and 6- C3177-200 non-treated.)

using both the sodium acetate treated and non-treated results. A t-test calculation performed on the respective data shows no significant differences among the three radio-tracer methods or between the sodium acetate treated and untreated samples. These results imply that the presence of small concentrations of carbonate minerals and coatings do not bias the CEC values measured by releasing calcium to compete with the tracers or by coating grain surfaces and reducing the number of available exchange sites.

Figure 4.10 is a graph of the total calculated CEC of samples from borehole C3177 as a function of depth utilizing the ^{85}Sr radio-tracer technique. In general, there is sufficient overlap of error bars indicating no measurable differences in CEC for the borehole samples as a function of depth. This result is not surprising based on the results of the particle size analysis (Table 4.1) and bulk sediment composition (Table 4.4), which indicate that the borehole samples are primarily composed of sand and have similar elemental and mineralogical compositions. The average CEC of all samples and replicates tested was 3.87 meq/100 g with a relative percent standard deviation of 15.7%. Overall, this indicates good agreement given the relatively small sample size (approximately 2 g) and the inherent heterogeneity of sediment samples. Furthermore, the calculated CECs in Figure 4.10 are consistent with the typical range (2 to 5 meq/100g) measured in Hanford site soils (Serne et al. 2002a).

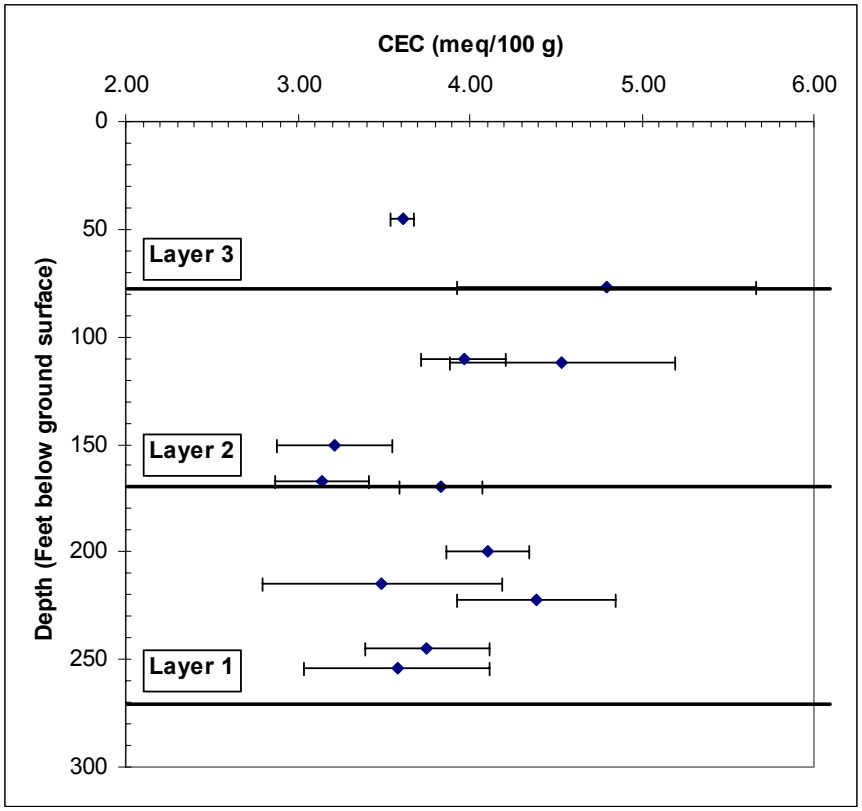

Figure 4.10. Calculated Cation Exchange Capacities of Borehole C3177 Samples

5.0 Summary and Conclusion

The physical and geochemical properties were characterized for six composite and six discrete depth samples from the second ILAW borehole C3177 (299-E24-21) to augment data previously collected for recharge studies and from borehole 299-E17-21, the first ILAW borehole. The composite samples will be used in future geochemical studies focused on determining interactions between Hanford formation sediments and contaminants that will leach from the glass waste forms scheduled to be disposed in the ILAW facility.

The particle-size distribution, moisture content, whole sediment chemical composition, carbon content, surface area, and mineralogy of the bulk and clay fractions were determined in the laboratory. Also analyzed were the pH, electrical conductivity, alkalinity, and the major and trace metal and anion concentrations of 1:1 sediment to water extracts.

All samples are sand or gravelly sand. Moisture content ranges from 1.7 to 5.3 wt. %. The bulk chemistry and mineralogy of the samples are typical of the Hanford formation sand-dominated sequence. Likewise, the chemical characteristics of the 1:1 water extracts are similar to extracts from other samples of the Hanford formation sand-dominated sequence from other boreholes. The water extracts (and by inference the natural vadose zone pore water) from borehole C3177 are dominated by sodium, calcium, magnesium, sulfate, and bicarbonate (from alkalinity).

No information was found by this characterization effort that would invalidate any of the data used in the 2001 performance assessment (Mann et al. 2001) of the overall performance of the proposed repository.

6.0 References

Anderson, B. J., and E. A. Jenne. 1970. "Free-Iron and Manganese Oxide Content of Reference Clays." *Soil Science*, v. 109, pp. 163-169.

ASTM D422-63. 1986. *Standard Test Method for Particle-Size Analysis of Soils*. Annual Book of ASTM Standards, American Society of Testing Material, Philadelphia, Pennsylvania.

ASTM D2216-98. 1986. *Test Method Laboratory Determination of Water (Moisture) Content of Soil, Rock, and Soil-Aggregate Mixtures.* Annual Book of ASTM Standards, American Society of Testing Material, Philadelphia, Pennsylvania.

ASTM D4129-88. 1988. *Standard Methods for Total and Organic Carbon in Water by High Temperature Oxidation and by Coulometric Detection*. Annual Book of ASTM Standards, American Society for Testing and Materials, West Conshohocken, Pennsylvania.

Babcock, K. L. and R. K. Schulz. 1970. "Isotopic and Conventional Determination of Exchangeable Sodium Percentage of Soil in Relation to Plant Growth." *Soil Science*, v. 109, pp 19-22.

Beetem, W. A., V. J. Janzer, and J. S. Wahlberg. 1962. *Use of Cesium-137 in the Determination of Cation Exchange Capacity.* Geological Survey Bulletin 1140-B, U.S. Department of the Interior, Washington D.C.

Brindley, G. W. 1980. "Quantitative X-ray Mineral Analysis of Clays*."* In *Crystal Structures of Clay Minerals and Their X-ray Identification,* (eds.) Brindley, G. W. and G. Brown, Monograph No. 5, Mineralogical Society, London.

Brunauer, S., P. H. Emmett, and E. Teller. 1938. "Adsorption of Gases in Multimolecular Laye*rs."* *J. Am. Chem. Soc.* v. 60, pp. 309-319.

Davis, J. A. and J. O. Leckie. 1978. "Surface Ionization and Complexation at the Oxide/Water Interface. II. Surface Properties of Amorphous Iron Oxyhydroxide and Adsorption of Metal Ions." *Jour. Colloid and Interface Science*, v. 67, pp. 90-107.

Dong, D., Y. M. Nelson, L. W. Lion, M. L. Shuler, and W. C. Ghiorse. 2000. "Adsorption of Pb and Cd onto Metal Oxides and Organic Material in Natural Surface Coatings as Determined by Selective Extractions: new Evidence for the Importance of Mn and Fe Oxides." *Water Resources*, v. 34-2, pp. 427-436.

Drever, J. I. 1973. "The Preparation of Oriented Clay Mineral Specimens for X-ray Diffraction Analysis by a Filter-membrane Peel Technique." *Amer. Minerl.* 58:553-554.

EPA. 1986. *Test Methods for Evaluating Solid Waste: Physical/Chemical Methods, SW-846, Third Edition*. Office of Solid Waste and Emergency Response, U.S. Environmental Protection Agency, Washington, D.C.

EPA. 1993. *Methods for the Determination of Inorganic Substances in Environmental Samples.* EPA-600/R-93-100, U.S. Environmental Protection Agency, Washington, D.C.

Folk, R. L. 1968. *Petrology of Sedimentary Rocks.* Hemphill, Austin, Texas.

Govindaraju, K. 1994. Geostandards Newsletter, vol. 18, Special Issue, p. 1-158.

Grim, R. E. 1968. *Clay Mineralogy.* 2nd edition. McGraw-Hill book Company, New York.

Joint Committee on Powder Diffraction Standards. 1974. *Search Manual for Selected Powder Diffraction Files for Mineral*: Joint Committee on Powder Diffraction Standards, Swarthmore, Pennsylvania.

Mann, F. M., K. C. Burgard, W. R. Root, P. E. LaMont, R. J. Puigh, S. H. Finfrock, R. Khaleel, D. H. Bacon, E. J. Freeman, B. P. McGrail, S. K. Wurstner. 2001. *Hanford Immobilized Low-Activity Waste Performance Assessment: 2001 Version*. DOE/ORP-2000-24, Revision 0 (formerly DOE/RL-97-69), U.S. Department of Energy, Richland, Washington.

McAlister, J. J., and B. J. Smith. 1999. "Selectivity of Ammonium Acetate, Hydroxylamine Hydrochloride, and Oxalic Ascorbic Acid Solutions for the Speciation of Fe, Mn, Zn, Cu, Ni, and Al in Early Tertiary Paleosols." *Microchem. Jour*., v. 63, pp. 415-426.

Moore, D. M. and R. C. Reynolds, Jr. 1989. *X-ray Diffraction and the Identification and Analysis of Clay Minerals*. Oxford University Press, New York.

Newman, A.C.D., and G. Brown. 1987. "The Chemical Constitution of Clays." In *Chemistry of Clays and Clay Minerals,* (ed.) A.C.D. Newman, Monograph No 6, Mineralogical Society, London.

PNL. 1990. *Procedures for Groundwater Investigations.* PNNL-MA-567, Pacific Northwest Laboratory, Richland, Washington

Reidel, S. P., D. G. Horton, and M. M. Valenta. 2001. *Geologic and Wireline Borehole Summary from the Second ILAW Borehole (299-E24-21).* PNNL-13652, Pacific Northwest National Laboratory, Richland, Washington.

Rhoades, J. D. 1996. "Salinity: Electrical Conductivity and Total Dissolved Solids." In *Methods of Soil Analysis Part 3.* J. M. Bigham (ed.), pp 417-435. American Society of Agronomy, Madison, Wisconsin.

Routson, R. C., R. E. Wildung, and R. J. Serne. 1973. "A Column Cation-Exchange-Capacity Procedure for Low-Exchange-Capacity Sands." *Soil Science*, v. 115, pp. 107-112.

Serne R., B. N. Bjornstad, H. T Schaef, B. A. Williams, D. C. Lanigan, D. G. Horton, R. E. Clayton, A. V. Mitroshkov, V. L. Legore, M. J. O'Hara, C. F. Brown, K. E. Parker, I. V. Kutnyakov, J. N. Serne, G. V. Last, S. C. Smith, C. W. Lindenmeier, J. M. Zachara, and D. Burke. 2002a. *Characterization of Vadose Zone Sediment: Uncontaminated RCRA Borehole Core Samples and Composite Samples*. PNNL-13757-1, Pacific Northwest National Laboratory, Richland, Washington.

Serne R. J., C. F. Brown, H. T. Schaef, E. M. Pierce, M. J. Lindberg, Z. Wang, P. L. Gassman, and J. G. Catalano. 2002b. *300 Area Uranium Leach and Adsorption Project*. PNNL-14022, Pacific Northwest National Laboratory, Richland, Washington

Tessier, A., P. G. C. Campbell, and M. Bisson. 1979. "Sequential Extraction Procedure for the Speciation of Particulate Trace Metals." *Anal. Chem*., v. 51-7, pp. 844-850.

USGS. 2001. "Alkalinity and Acid Neutralizing Capacity." Book 9, In *National Filed Manual for the Collection of Water-Quality Data*, (eds.) S. A. Rounds and F. D. Wilde, U.S. Geological Survey, Washington D.C. Available at http://water.usgs.gov/owq.

Walker, L. D. 2001. *Borehole Summary Report for the 2001 ILAW Site Characterization Well.* BHI-01531, Bechtel Hanford, Inc., Richland, Washington.

Wentworth, C. K. 1922. "A Grade Scale and Class Terms for Clastic Sediment." *J. Geol.*, v. 30, pp. 377-392.

Appendix A

Additional Data from Borehole C3177 Samples

Appendix A

Additional Data from Borehole C3177 Samples

This appendix contains additional data and information about the borehole C3177 samples. Figure A.1 shows bulk sediment diffraction patterns for each of the characterized samples. Mineral identification was based on the 2θ position of the main reflections for each mineral. The main quartz reflection is at 26.63° 2θ, followed by less intense reflections at 20.86, 36.53, 39.46, 42.43, 50.12, and 59.92° 2θ. The main reflections associated with feldspar minerals are between 27.34° 2θ and 27.92° 2θ, with the higher 2θ values belonging to the plagioclase series. Chlorite and mica minerals were identified by reflections at 6.3° 2θ and 8.8° 2θ, respectively. The presence of an amphibole was established by the characteristic 100% reflection at 10.5° 2θ. Additionally, trace amounts of the zeolite, laumontite, were identified in most of the samples by a diffraction peak positioned at 9.36° 2θ.

Figure A.2 shows diffraction patterns for the Mg-saturated, ethylene glycol solvated specimen from each borehole sample. Smectite was identified by a shift in the 5.85° 2θ basal reflection on the diffraction pattern of the Mg-saturated specimen to 5.28° 2θ after solvation with ethylene glycol. Saturation with K^+ causes the reflection to shift to 7.3° 2θ and heating the sample at 575° for one hour causes the main smectite reflection to irreversibly collapse to 8.88° 2θ.

The basal reflections for illite (mica) are at 8.88, 17.8, and 26.7° 2θ. Cation saturation, solvation with ethylene glycol, and heating do not affect the position of these reflections. An increase in intensity of the 8.88° 2θ reflection.

Chlorite is identified by a series of basal reflections at 6.24, 12.5, 18.8, and 25.2° 2θ, which are unaffected by cation saturation or ethylene glycol solvation. Heating to 575°C shifts the first order reflection to 6.37° 2θ and tends to diminish or eliminate the intensity of the higher order reflections (12.5, 18.8, and 25.2° 2θ).

Kaolinite is difficult to identify in the presence of chlorite. Basal reflections characteristic of kaolinite are at 12.5 and 24.9° 2θ and are superimposed on the even-ordered chlorite reflections. Kaolinite reflections are unaffected by cation saturation and ethylene glycol solvation. Heating the specimen to 575°C destroys the crystallinity of the kaolinite structure and the kaolinite reflections are eliminated. Positive identification of kaolinite in the presence of chlorite can be made by differentiating the kaolinite basal reflection at 24.9° 2θ from the chlorite reflection at 25.2° 2θ.

Trace amounts of quartz in the <1.4 μm fractions are evident by the diffraction peak located at 20.85° 2θ. The 100% reflection for quartz (26.6° 2θ) is hidden by the third-order basal reflection of illite located at 26.6° 2θ. Plagioclase feldspar is also identified in the clay fractions by the minor diffraction peak at 27.8° 2θ.

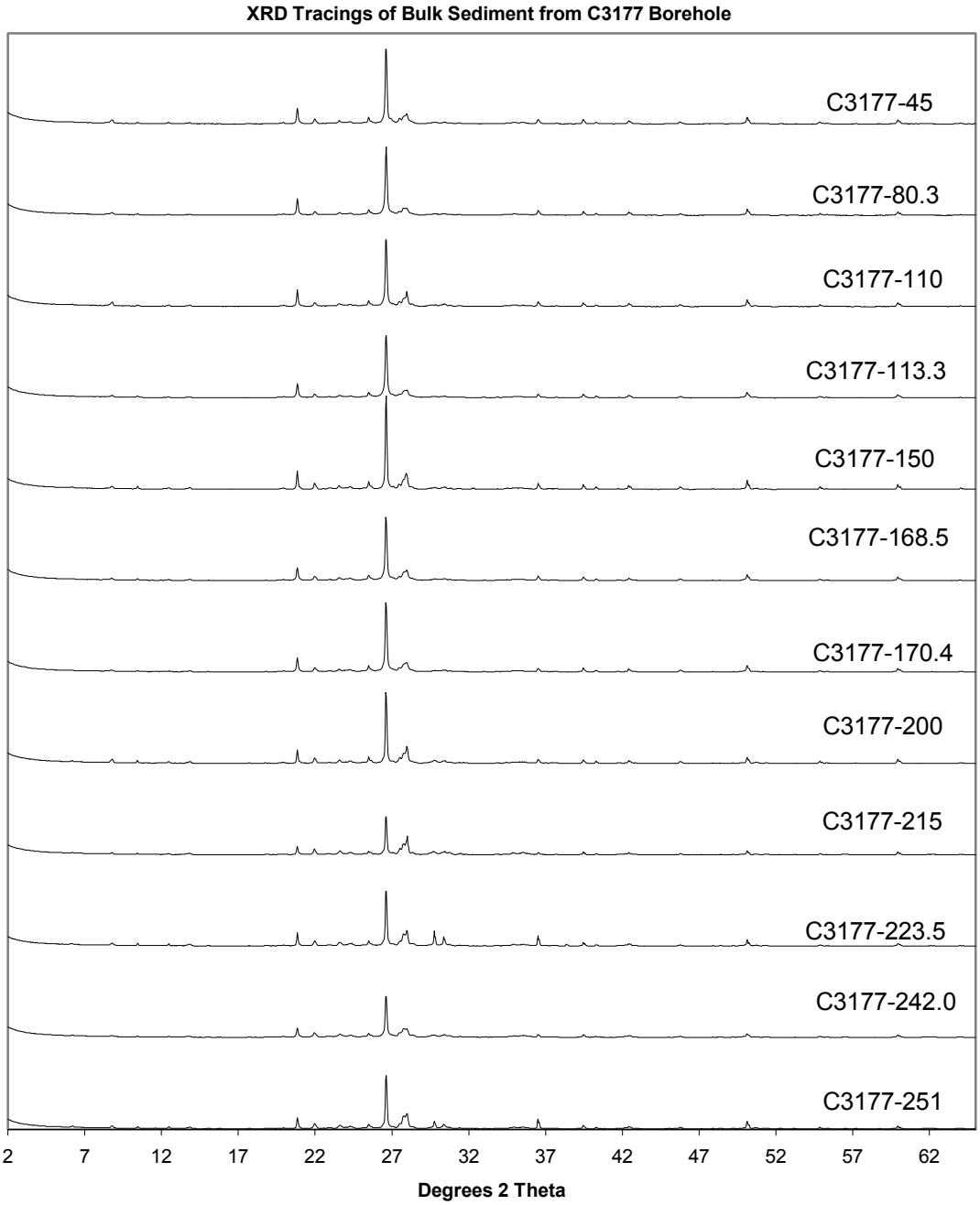

Figure A.1. X-Ray Diffraction Patterns of Bulk Sediment from Borehole C3177

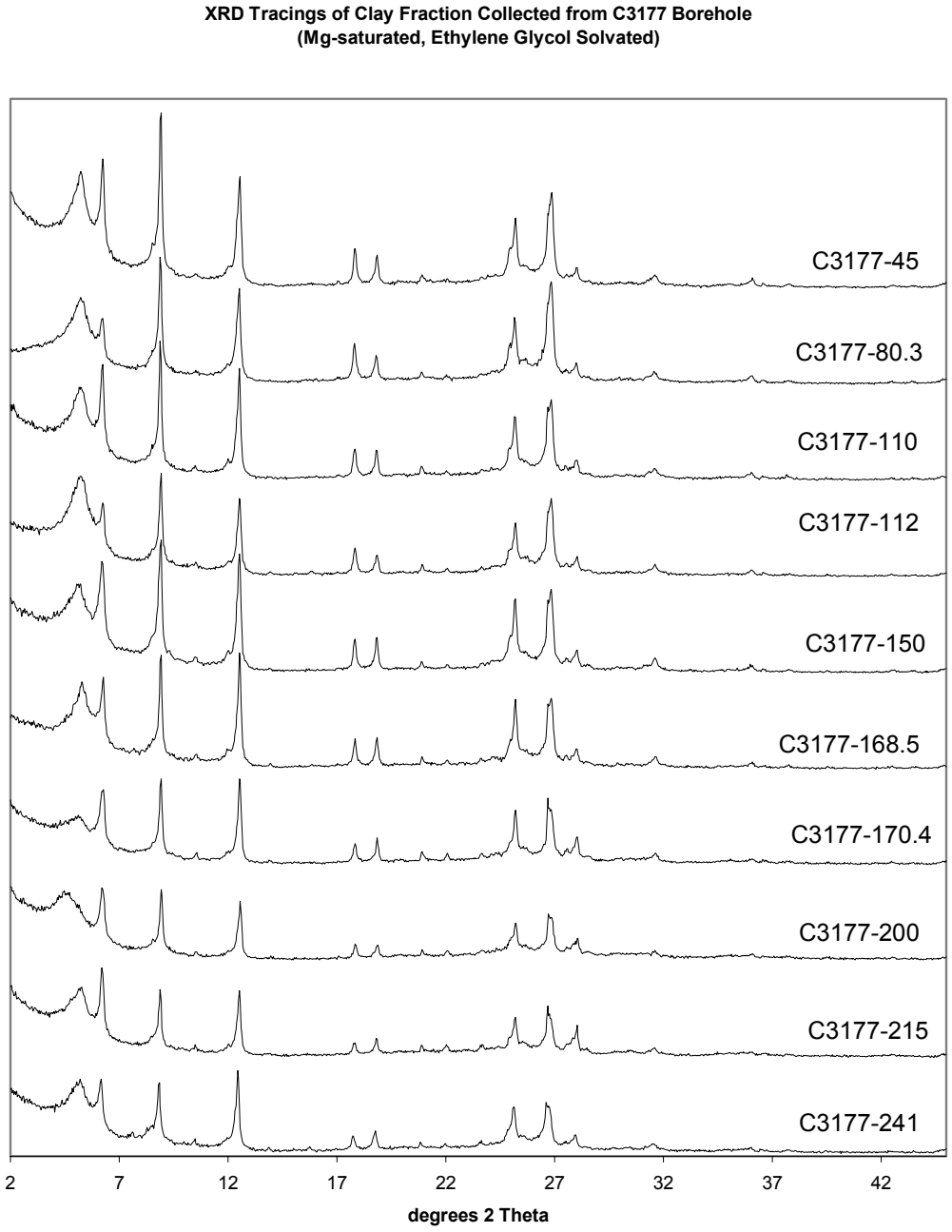

Figure A.2. X-Ray Diffraction Patterns of Mg-Saturated, Ethylene Glycol Solvated Specimens from Borehole C3177

In addition to x-ray diffraction (XRD) transmission electron microscopy (TEM) characterization of selected clay-size samples was conducted using a JEOL 1200X electron microscope equipped with a Links detector system. Although such detailed characterization is probably not significant to the ILAW Performance Assessment, the information gleaned from the TEM analyses may be useful in studies of contaminant movement through the vadose zone.

Samples were prepared for TEM analyses by transferring a small aliquot of dilute clay slurry onto a formvar carbon coated 3-mm copper support grid. The clay solution contained 0.15% tert-butylamine to reduce the surface tension of water.

Structural formulas were derived from data collected from the TEM analysis. On average, an energy dispersive x-ray spectra was collected from a minimum of five particles from the same mineral phase common to the sample. Pure minerals from the Clay Mineral Society's Reference clay Repository were used as standards. The x-ray spectra were collected and processed using the Cliff-Lorimer Ratio Thin Section method and then converted to a structural formula (based on half-unit cell ($O_{10}(OH)_2$) by the method described in Moore and Reynolds (1989) and Newman and Brown (1987).

Examination of samples C3177-80.3 and C3177-251 by TEM allowed detailed characterization of the various clay minerals identified by XRD. Overall illite and chlorite particles dominated the coarser component of the clay fractions with individual grain sizes commonly measuring 1 to 4 μm in length. Figure A.3 is an example of a representative illite particle measuring approximately 4 μm in length. The

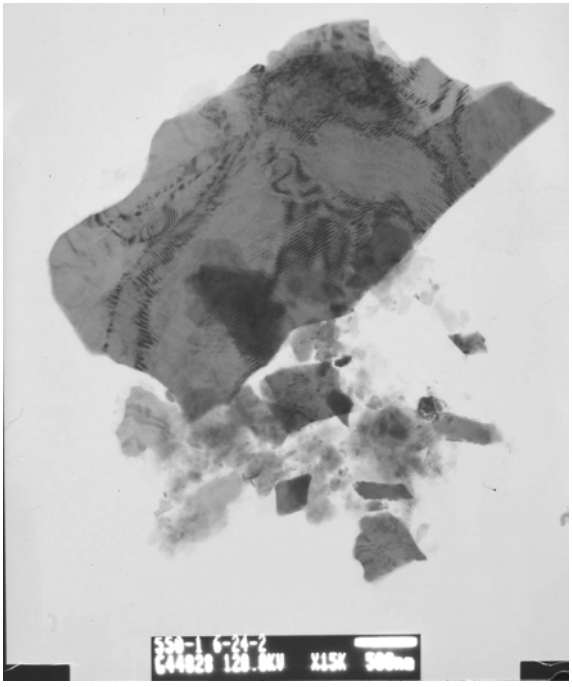

Figure A.3. Large Illite Particle from Sample C3177-80.3. The particle is about 4 μm in length.

particle exhibits a thin platy habit making it easily distinguishable from other clay minerals. Using data from TEM analysis and assuming all iron is present as Fe^{3+}, the following structural formula was estimated to be:

$$[K^{+}_{0.63}Ca^{2+}_{0.01}]^{+0.65}[(Al^{3+}_{1.58}Mg^{2+}_{0.30}Fe^{3+}_{0.21}Ti^{4+}_{0.02})^{+0.05}(Si^{4+}_{3.29}Al^{3+}_{0.71})^{-0.71}]^{-0.64}O_{10}(OH)_2 \qquad [1]$$

As in muscovite, the layer charge for the illite originates in the tetrahedral sheet (-0.71), with a slight positive contribution from the octahedral sheet (+0.05), resulting in a 2:1 layer charge of –0.64. The interlayer charge of +0.65 balances the charge on the 2:1 silicate structure. Iron content of eight illite particles examined by TEM ranged between 0.08 and 0.54 atoms per $O_{10}(OH)_2$ and octahedral Al^{3+} ranged between 1.07 and 1.70 atoms per $O_{10}(OH)_2$. Traces of Ti^{+4} were detected in most of the illites.

Chlorite particles display platy habits and often appeared similar in shape and texture to illite. Figure A.4 is an example of a typical chlorite particle approximately 1 μm in size found in the clay

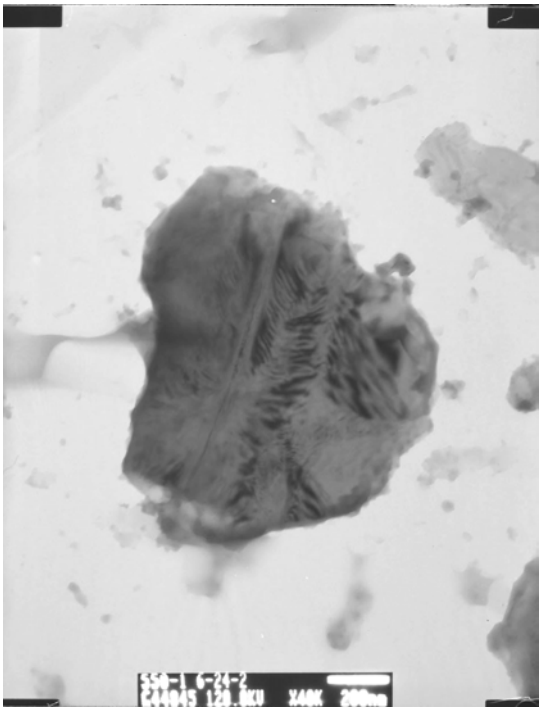

Figure A.4. Chlorite Aggregate from Sample C3177-251. The aggregate is a little over one micron in size.

fraction of sample C3177-251. Chlorite particles were found to be generally smaller than illite particles with sizes ranging between 1 to 2 μm. An estimated structural formula for this particular particle from TEM data is the following:

$$\left[K^{+}_{0.01}\right]^{+0.01}\left[(Al^{3+}_{1.45}Mg^{2+}_{2.90}Fe^{2+}_{1.44})^{+1.03}(Si^{4+}_{2.92}Al^{3+}_{1.08})^{-1.08}\right]^{-0.05}O_{10}(OH)_8. \qquad [2]$$

The structural formula shows the negative charge in the tetrahedral sheet, originating from the substitution of Al^{3+} for Si^{4+}, is balanced by the inclusion of the trivalent cation, Al^{3+}, and divalent cations, Mg^{2+} and Fe^{2+} into the octahedral sheets. The total number of cations occupying octahedral sites is 5.79 per $O_{10}(OH)_8$. TEM analysis of four individual chlorite grains showed Fe^{2+} concentrations ranging from 0.96 to 1.44 atoms per $O_{10}(OH)_8$ and Mg^{2+} ranging from 2.90 to 3.26 atoms per $O_{10}(OH)_8$. Small amounts of K^{+} were included in the structural formula, but are most likely from very small illite grains that could not be separated from the chlorite grains during the analysis.

Smectite dominates the finer particles of the clay fractions. Smectite is typically found as fine-grained flakes in the <0.5 μm range and occasionally as aggregates up to 1 to 2 μm in size. Figure A.5 is an example of several dense smectite aggregates measuring less than 2 μm. The aggregates consist of a dense center from which delicate thin films of individual smectite flakes extend outward. These individual films can be seen curling up around the edge of the aggregate.

Figure A.5. TEM Photomicrograph of the Clay Fraction of Sample C3177-80.3. TEM shows the morphology of individual smectite aggregates.

Although individual smectite flakes or aggregates were never sufficiently isolated during the TEM analysis to obtain data for developing a structural formula, using data collected by energy dispersive spectroscopy during TEM analysis showed smectite aggregates to be rich in iron, with minor amounts of magnesium and aluminum. The iron concentrations were consistent from particle to particle, but the magnesium and aluminum concentrations varied.

Crystalline phases not detected in the XRD analysis, but observed by TEM, included various oxides of chromium, iron, manganese, and titanium. These oxides were associated with the finest grain-size fractions and are generally <0.1 μm in size. Additionally, individual rhomboid shaped grains of apatite (calcium phosphate) were found throughout the sample.

Tables A.1 and A.2 give the complete chemical analyses obtained by inductively coupled plasma optical emissions spectroscopy (ICP-OES) and by inductively coupled plasma mass spectroscopy (ICP-MS). These data are discussed in the main body of this report. Table A.3 gives the complete data set resulting from the iron extraction experiments. Tables A.4 , A.5, and A.6 give the results of the cation exchange experiments using ^{22}Na, ^{137}Cs, and ^{85}Sr. Table A.7 is the total calculated cation exchange capacity of samples using the ^{85}Sr radio-tracer technique.

Table A.1. Metal Concentrations in Samples from Borehole C3177 Determined by ICP-OES[(a)]

Analyte Sample Number	Al (μg/L)	As (μg/L)	B (μg/L)	Ba (μg/L)	Be (μg/L)	Bi (μg/L)	Ca (μg/L)	Cd (μg/L)	Co (μg/L)	Cr (μg/L)	Cu (μg/L)
C3177-45	41	24	(38)	23	(2.2)	ND	7,825	(1.3)	(2)	(1.1)	(25)
C3177-80.3	ND	12	(30)	14	(0.5)	(3)	27,766	(0.4)	(1)	(0.9)	(5)
C3177-110	45	24	(35)	21	(1.6)	ND	5,795	(1.1)	(2)	(1.1)	(21)
C3177-113.3	(9)	20	(33)	19	(0.5)	(2)	13,207	(0.5)	(1)	(0.9)	(7)
C3177-150	39	20	(33)	14	(1.2)	ND	7,548	(0.6)	(1)	(0.7)	(16)
C3177-168.5	37	20	(30)	17	(0.5)	ND	6,943	(0.2)	(1)	(0.7)	(6)
C3177-170.4	60	14	(37)	18	(0.3)	ND	8,745	(0.3)	ND	(0.5)	(4)
C3177-200	34	16	(30)	15	(0.9)	(1)	8,663	(0.5)	(1)	(0.7)	(12)
C3177-215	43	(6)	(27)	39	(0.7)	ND	11,995	(0.5)	(1)	(0.7)	(10)
C3177-223.5	(22)	(6)	(26)	26	(0.2)	(2)	10,702	(0.1)	(1)	(0.5)	(3)
C3177-242	56	10	(24)	15	(0.2)	ND	2,809	(0.1)	(1)	(0.3)	(4)
C3177-251	50	(7)	(27)	21	(0.6)	(1)	13,528	(0.5)	(1)	(0.7)	(8)

Table A.1. (Cont.)

Analyte Sample Number	Fe (µg/L)	K (µg/L)	Mg (µg/L)	Mn (µg/L)	Mo (µg/L)	Ni (µg/L)	P (µg/L)	Pb (µg/L)	Se (µg/L)	Sr (µg/L)	Zn (µg/L)
C3177-45	30	5,356	3,370	3.4	10	(10)	(55)	(12)	(3)	43	31
C3177-80.3	41	3,716	1,880	2.9	9	(6)	(54)	(20)	ND	28	49
C3177-110	27	3,390	2,305	(2.0)	11	(7)	(56)	(18)	(3)	40	27
C3177-113.3	21	4,551	2,963	(2.0)	8	(7)	(42)	(6)	(5)	45	29
C3177-150	20	5,341	3,985	(2.2)	7	(6)	(22)	(18)	(4)	67	29
C3177-168.5	25	4,511	4,072	(1.3)	7	(6)	(24)	(16)	(8)	67	24
C3177-170.4	16	7,481	11,539	(0.4)	12	(4)	(36)	(2)	(13)	125	28
C3177-200	11	3,758	4,003	(0.8)	10	(5)	(77)	(17)	(5)	52	27
C3177-215	29	2,941	2,008	(0.9)	8	(7)	(62)	(7)	ND	34	26
C3177-223.5	25	5,216	2,684	(1.9)	16	(5)	(75)	(19)	(4)	50	31
C3177-242	15	4,775	3,665	(0.5)	(4)	(3)	(19)	(11)	(1)	55	29
C3177-251	52	2,862	927	(1.4)	(3)	(3)	(70)	(24)	(1)	16	35

Analyte Sample Number	Na (µg/L)	Si (µg/L)	S (µg/L)	Ti (µg/L)	Zr (µg/L)
C3177-45	19,032	9,384	11,547	(3)	(2)
C3177-80.3	15,841	10,059	28,780	(3)	(2)
C3177-110	10,264	7,469	4,385	(2)	(1)
C3177-113.3	14,926	10,328	8,854	(2)	(1)
C3177-150	15,349	9,748	3,740	(2)	(1)
C3177-168.5	13,436	8,460	3,991	(2)	(1)
C3177-170.4	20,101	10,179	5,055	(1)	ND
C3177-200	13,739	7,884	9,537	(1)	ND
C3177-215	11,470	7,023	17,154	(2)	ND
C3177-223.5	19,429	7,658	13,975	(1)	(1)
C3177-242	15,105	9,892	1,600	(1)	(1)
C3177-251	18,810	11,150	15,968	(2)	ND

(a) Values in parentheses are less than the limit of quantitation.
ND = Not detected.

Table A.2. Metal Concentrations in Samples from Borehole C3177 Determined by ICP-MS[(a)]

Analyte / Sample Number	Tc 99 (µg/l)	U 238 (µg/l)	Cr 52 (µg/l)	Cr 53 (µg/l)	As 75 (µg/l)	Se 82 (µg/l)	Mo 95 (µg/l)	Mo 98 (µg/l)
C3177-45	(0.01)	0.297	(0)	(0.5)	16.2	1.64	4.18	3.91
C3177-80.3	(0.01)	0.561	(1)	3.74	11.5	5.63	7.81	7.13
C3177-110	(0.01)	0.266	(0)	(0.4)	18.9	0.537	4.41	4.02
C3177-113.3	(0.01)	0.464	(1)	(1.3)	15.2	1.44	8.10	7.37
C3177-150	(0.01)	0.332	(0)	(0.6)	17.9	(0.35)	7.42	6.81
C3177-168.5	(0.01)	0.417	(1)	(0.5)	18.7	0.507	6.41	5.87
C3177-170.4	(0.01)	0.428	(1)	(1.4)	15.0	<0.500	14.7	13.6
C3177-200	(0.01)	0.386	(0)	(0.4)	11.1	<0.500	4.72	4.29
C3177-215	(0.00)	0.239	(0)	(0.2)	6.11	2.77	3.76	3.38
C3177-223.5	(0.01)	0.236	(0)	(0.4)	7.87	3.18	3.37	3.03
C3177-242	(0.01)	0.270	(1)	(0.2)	10.0	(0.34)	2.30	2.09
C3177-251	(0.01)	0.303	(0)	(0.2)	7.30	3.24	3.89	3.62

Analyte / Sample Number	Mo 100 (µg/l)	Ru 101 (µg/l)	Ru 102 (µg/l)	Ru 104 (µg/l)	Ag107 (µg/l)	Ag 109 (µg/l)	Cd 111 (µg/l)	Cd 114 (µg/l)	Pb 206 (µg/l)	Pb 208 (µg/l)
C3177-45	1.87	<0.250	<0.100	<0.100	<0.500	<0.500	<0.250	<0.100	<1.00	<1.00
C3177-80.3	1.92	<0.250	<0.100	(0.00)	<0.500	<0.500	(0.02)	(0.00)	(0.08)	(0.08)
C3177-110	3.26	<0.250	<0.100	<0.100	<0.500	<0.500	<0.250	<0.100	<1.00	<1.00
C3177-113.3	2.05	<0.250	<0.100	<0.100	<0.500	<0.500	(0.00)	(0.00)	<1.00	<1.00
C3177-150	1.63	<0.250	<0.100	(0.00)	<0.500	<0.500	<0.250	<0.100	<1.00	<1.00
C3177-168.5	1.74	<0.250	<0.100	(0.01)	<0.500	<0.500	<0.250	<0.100	<1.00	<1.00
C3177-170.4	3.45	<0.250	<0.100	(0.04)	<0.500	<0.500	<0.250	<0.100	<1.00	<1.00
C3177-200	3.50	<0.250	<0.100	(0.01)	<0.500	<0.500	(0.02)	(0.00)	(0.36)	(0.38)
C3177-215	2.84	<0.250	<0.100	(0.01)	<0.500	<0.500	(0.02)	(0.00)	(0.02)	(0.01)
C3177-223.5	6.65	(0.05)	(0.03)	(0.08)	<0.500	<0.500	(0.17)	(0.06)	(0.42)	(0.26)
C3177-242	1.48	(0.07)	(0.05)	(0.09)	(0.00)	(0.01)	(0.17)	(0.08)	(0.41)	(0.23)
C3177-251	1.06	(0.07)	(0.04)	(0.06)	<0.500	<0.500	(0.14)	(0.06)	(0.84)	(0.75)

(a) Values in parentheses are less than the limit of quantitation.

Table A.3. Iron Oxide Data from Borehole C3177 Samples

Sample Number [(a)]	Tare (g)	With Soil (g)	Soil Wt. (g)	Dry Wt. (g)	Total Wt. (g)	Sol. Wt. (g)	Density Correction	Sol. Vol. (mL)	Fe Conc. (µg/L)	Fe Total (µg)	Fe Removed (µg/g)	Avg Fe (µg/g)
C3177-45-1 H-HCl	32.32	37.39	5.07	4.97	144.99	107.70	1.0452	103.04	48,421	4,989	1,003	1,095
C3177-45-2 H-HCl	32.26	37.24	4.98	4.89	142.02	104.87	1.0452	100.34	57,826	5,802	1,187	
C3177-45-1 Tamms	40.38	45.38	5.00	4.91	248.94	203.65	1.0099	201.66	32,919	6,638	1,353	1,240
C3177-45-2 Tamms	40.09	45.14	5.05	4.95	249.99	204.95	1.0099	202.94	27,501	5,581	1,126	
C3177-45-1 HCO	32.32	37.3	4.98	4.89	150.52	113.31	1.0976	103.24	101,955	10,526	2,154	2,093
C3177-45-2 HCO	32.31	37.32	5.01	4.92	148.73	111.50	1.0976	101.59	98,329	9,989	2,032	
C3177-45-1 SD	32.19	37.27	5.08	4.98	144.80	107.63	1.0766	99.97	136,926	13,688	2,746	2,772
C3177-45-2 SD	32.21	37.22	5.01	4.92	149.65	112.52	1.0766	104.52	131,612	13,756	2,798	
C3177-110-1 H-HCl	32.15	37.13	4.98	4.92	143.14	106.07	1.0452	101.49	52,271	5,305	1,079	1,099
C3177-110-2 H-HCl	32.22	37.23	5.01	4.94	139.10	101.94	1.0452	97.53	56,670	5,527	1,118	
C3177-110-1 Tamms	40.77	45.86	5.09	5.02	248.93	203.14	1.0099	201.14	40,319	8,110	1,614	1,378
C3177-110-2 Tamms	39.88	44.99	5.11	5.04	247.67	202.75	1.0099	200.76	28,688	5,759	1,142	
C3177-110-1 HCO	32.49	37.48	4.99	4.93	153.77	116.35	1.0976	106.01	94,897	10,060	2,043	1,988
C3177-110-2 HCO	32.14	37.19	5.05	4.98	146.38	109.26	1.0976	99.54	96,834	9,639	1,934	
C3177-110-1 SD	32.18	37.21	5.03	4.96	146.64	109.50	1.0766	101.7	134,503	13,680	2,755	2,789
C3177-110-2 SD	32.35	37.5	5.15	5.08	144.53	107.10	1.0766	99.48	144,196	14,344	2,822	
C3177-200-1 H-HCl	32.18	37.23	5.05	4.99	143.30	106.13	1.0452	101.54	53,985	5,482	1,099	1,086
C3177-200-2 H-HCl	32.2	37.25	5.05	4.99	141.78	104.59	1.0452	100.07	53,486	5,352	1,073	
C3177-200-1 Tamms	40.72	45.73	5.01	4.95	252.18	206.51	1.0099	204.49	46,527	9,514	1,923	1,809
C3177-200-2 Tamms	40.37	45.39	5.02	4.96	248.90	203.57	1.0099	201.58	41,686	8,403	1,695	
C3177-200-1 HCO	32.29	37.36	5.07	5.01	149.31	112.01	1.0976	102.05	106,427	10,861	2,169	2,093
C3177-200-2 HCO	32.19	37.26	5.07	5.01	149.20	112.00	1.0976	102.04	98,908	10,093	2,016	
C3177-200-1 SD	32.13	37.18	5.05	4.99	149.10	111.98	1.0766	104.02	127,207	13,231	2,653	2,798
C3177-200-2 SD	32.36	37.39	5.03	4.97	146.84	109.51	1.0766	101.72	143,707	14,618	2,943	

(a) H-HCl corresponds to the hydroxylamine hydrochloride extraction solution, Tamms corresponds to the ammonium oxalate/oxalic acid extraction solution, HCO corresponds to the sodium dithionite/sodium bicarbonate extraction solution, and SD corresponds to the sodium dithionite/citric acid extraction solution.

Table A.4. Cation Exchange Capacity Calculations Using ^{22}Na Radio-Isotope Exchange Method

Sample Description	Soil cpm	Soil Wt (g)	Soil Activity (cpm/g)	Solution Activity (cpm)	Solution (cpm/meq)	CEC (meq/100 g)	Average CEC
C3177-45 w/NaOAc	9,047	2.1	4,247	5,986	148,727	2.9	2.8
C3177-45 w/NaOAc	8,458	2.0	4,272	6,195	153,039	2.8	
C3177-45	9,024	2.5	3,683	5,443	130,400	2.8	2.5
C3177-45	7,843	2.3	3,410	6,472	157,278	2.2	
C3177-110 w/NaOAc	12,146	2.4	5,125	5,201	123,668	4.1	3.9
C3177-110 w/NaOAc	12,957	2.5	5,101	5,991	137,832	3.7	
C3177-110	9,991	2.4	4,146	5,635	135,708	3.1	3.1
C3177-110	10,831	2.5	4,421	5,786	137,591	3.2	
C3177-200 w/NaOAc	10,758	2.4	4,520	5,512	133,265	3.4	3.2
C3177-200 w/NaOAc	11,242	2.7	4,211	5,351	136,570	3.1	
C3177-200	12,668	2.6	4,798	5,213	127,565	3.8	3.4
C3177-200	10,324	2.4	4,375	5,755	141,245	3.1	

Table A.5. Cation Exchange Capacity Calculations Using ^{137}Cs Radio-Isotope Exchange Method

Sample Description	Soil cpm	Soil Wt (g)	Soil Activity (cpm/g)	Solution Activity (cpm)	Solution (cpm/meq)	CEC (meq/100 g)	Average CEC
C3177-45 w/NaOAc	28,618	1.9	15,190	16,866	421,648	3.6	3.4
C3177-45 w/NaOAc	31,153	2.3	13,803	17,659	441,483	3.1	
C3177-45	33,258	2.2	14,934	16,980	424,500	3.5	3.4
C3177-45	27,754	2.0	14,146	16,975	424,365	3.3	
C3177-110 w/NaOAc	35,889	2.3	15,476	16,620	415,500	3.7	3.7
C3177-110 w/NaOAc	34,292	2.3	15,107	16,653	416,313	3.6	
C3177-110	31,855	2.0	16,056	17,051	426,263	3.8	3.6
C3177-110	29,225	2.0	14,305	16,585	414,618	3.5	
C3177-200 w/NaOAc	31,782	2.3	13,812	17,333	433,333	3.2	3.6
C3177-200 w/NaOAc	34,868	2.2	16,046	16,296	407,408	3.9	
C3177-200	40,582	2.5	16,370	16,153	403,828	4.1	4.0
C3177-200	35,370	2.4	14,987	15,292	382,308	3.9	

Table A6. CEC Calculations Utilizing ^{85}Sr radio-Isotope Exchange Method

Sample Description	Soilcpm	Soil Wt (g)	Soil Activity (cpm/g)	Solution Activity (cpm)	Solution (cpm/meq)	CEC (meq/100 g)	Average CEC
C3177-45 w/NaOAc	81,063.7	2.13	38,076.0	95,359.7	1,191,996	3.2	3.22
C3177-45 w/NaOAc	81,751.7	2.13	38,399.1	94,880.4	1,186,005	3.2	
C3177-45	81,988.9	2.38	34,521.6	92,199.7	1,152,496	3.0	3.25
C3177-45	84,999.1	2.18	39,026.2	88,878.9	1,110,986	3.5	
C3177-110 w/NaOAc	82,864.7	2.13	38,867.1	94,371.4	1,179,643	3.3	3.27
C3177-110 w/NaOAc	81,371.1	2.26	36,004.9	88,538.0	1,106,725	3.3	
C3177-110	106,858.3	2.52	42,454.6	91,322.1	1,141,526	3.7	3.56
C3177-110	101,423.4	2.6	39,069.1	92,138.5	1,151,731	3.4	
C3177-200 w/NaOAc	80,533.4	2.36	34,124.3	89,738.2	1,121,728	3.0	3.36
C3177-200 w/NaOAc	83,702.5	2.24	37,333.9	40,543.7	1,013,593	3.7	
C3177-200	85,426.1	2.37	36,044.8	91,968.4	1,149,605	3.1	3.19
C3177-200	89,808.1	2.47	36,374.3	89,796.1	1,122,451	3.2	

Table A.7. Cation Exchange Capacity Data from Borehole C3177 Samples

Sample Description	Soil cpm	Soil Wt (g)	Soil Wt (g) Corrected	Soil Activity (cpm/g)	Solution Activity (cpm)	Solution (cpm/meq)	CEC (meq/ 100 g)	Average CEC
C3177-45 et al.	11,699	2.2	2.15	5,318	11,626	145,321	3.7	3.6
C3177-45 et al. Dup	11,646	2.32	2.27	5,020	11,268	140,850	3.6	
C3177-45/54 (or 200 et al.)	11,428	2.07	2.03	5,521	11,230	140,373	3.9	4.1
C3177-45/54 (or 200 et al.) Dup	14,276	2.32	2.28	6,154	11,527	144,085	4.3	
C3177-77	16,589	2.12	2.02	7,825	11,579	144,734	5.4	4.8
C3177-77 Dup	13,637	2.23	2.12	6,115	11,708	146,345	4.2	
C3177-110 et al.	13,288	2.38	2.31	5,583	11,781	147,263	3.8	4.0
C3177-110 et al. Dup	13,196	2.29	2.23	5,762	11,140	139,255	4.1	
C3177-112	17,466	2.26	2.12	7,728	12,368	154,601	5.0	4.5
C3177-112 Dup	14,971	2.42	2.27	6,187	12,153	151,918	4.1	
C3177-150/154	12,269	2.41	2.34	5,091	11,783	147,281	3.5	3.2
C3177-150/154 Dup	9,345	2.13	2.07	4,387	11,770	147,123	3.0	
C3177-167	10,791	2.48	2.41	4,351	11,788	147,353	3.0	3.1
C3177-167 Dup	10,850	2.2	2.14	4,932	11,834	147,924	3.3	
C3177-170	12,374	2.34	2.24	5,288	11,550	144,374	3.7	3.8
C3177-170 Dup	13,297	2.29	2.19	5,806	11,600	144,995	4.0	
C3177-215 et al.	13,493	2.34	2.3	5,766	11,584	144,798	4.0	3.5
C3177-215 et al. Dup	8,425	1.99	1.96	4,234	11,302	141,276	3.0	
C3177-222	17,134	2.61	2.55	6,565	11,141	139,259	4.7	4.4
C3177-222 Dup	13,162	2.3	2.25	5,723	11,274	140,920	4.1	
C3177-241	11,206	2.27	2.22	4,936	11,295	141,193	3.5	3.8
C3177-241 Dup	14,213	2.62	2.57	5,425	10,829	135,359	4.0	
C3177-251 et al.	13,437	2.51	2.46	5,353	10,814	135,170	4.0	3.6
C3177-251 et al. Dup	10,404	2.23	2.18	4,665	11,683	146,035	3.2	

References

Moore, D. M. and R. C. Reynolds, Jr. 1989. *X-ray Diffraction and the Identification and Analysis of Clay Minerals*. Oxford University Press, New York.

Newman, A.C.D., and G. Brown. 1987. "The Chemical Constitution of Clays." In *Chemistry of Clays and Clay Minerals,* (ed.) A.C.D. Newman, Monograph No 6, Mineralogical Society, London.

Appendix B

Electrical Charge Balance and Sulfur Balance

Appendix B

Electrical Charge Balance and Sulfur Balance

The charge balance of the major cations and anions was calculated to evaluate the internal consistency of the data sets. Cation concentrations from the inductively coupled plasma optical emissions spectroscopy (ICP-OES) and anion concentrations from the anion analyses were converted to concentrations in terms of milliequivalents/L and compared. This comparison was done only for the composite samples because alkalinity was not measured on the discrete-depth samples. The results are in Table B.1 of this appendix.

Generally, a charge balance within about 10% of zero net charge is considered very good for this type of data set. One half of the samples in Table B.1 have a calculated charge balance in this range. Of the other three, two are very close. The sample from 110 feet (ft) below ground surface (bgs) shows a charge unbalance of 20%. This indicates that either one or more analytes from the ICP-OES and/or IC measurements are in error or that there are substantial amounts of one or more cations or anions that were not included in the analysis.

As a second check between the data sets, the sulfate concentrations in the water extracts were calculated from the analyzed sulfur concentration measured by ICP-OES. The calculated sulfate concentrations were then compared with the measured concentrations from the IC analyses. These results are shown in Table B.2 of this appendix.

The calculated and measured sulfate concentrations for one half of the 12 samples are within about 10% of each other, and all but 2 samples are within 15%. These results are considered good. The results for the sample from 242 ft bgs are very different and indicate that either the sulfur value from the ICP-OES analysis or the sulfate value from the IC analysis is questionable.

Table B.1. Charge Balance for Composite Samples from Borehole C3177

Sample Number	Bicarbonate (from Alkalinity (meq/L)	Chloride (meq/L)	Nitrate (meq/L)	Sulfate (meq/L)	Sodium (meq/L)	Magnesium (meq/L)	Potassium (meq/L)	Calcium (meq/L)	Σ Anions (meq/L)	Σ Cations (meq/L)	Charge Balance (%)
C3177-45	0.52	0.12	0.04	0.65	0.83	0.28	0.14	0.39	1.33	1.63	10.06
C3177-110	0.49	0.09	0.01	0.24	0.69	0.15	0.10	0.29	0.82	1.23	19.90
C3177-150	0.55	0.10	0.01	0.20	0.45	0.19	0.09	0.38	0.86	1.10	12.11
C3177-200	0.49	0.07	0.01	0.52	0.65	0.24	0.12	0.43	1.09	1.44	13.78
C3177-215	0.53	0.04	0.02	1.18	0.67	0.33	0.14	0.60	1.77	1.73	-1.12
C3177-251	0.49	0.04	0.08	1.11	0.58	0.34	0.12	0.67	1.72	1.71	-0.01

Table B.2. Calculated and Measured Sulfate for Samples from Borehole C3177

Sample Number	ICP-OES		IC
	Measured Sulfur	Calculated Sulfate	Measured Sulfate
	µg/L		
C3177-45	11,547	34,641	31,260
C3177-80.3	28,780	86,340	74,750
C3177-110	4,358	13,155	11,730
C3177-113.3	8,854	26,562	29,760
C3177-150	3,740	11,220	9,760
C3177-168.5	3,991	11,973	9,960
C3177-170.4	5,055	15,165	16,030
C3177-200	9,537	28,611	24,830
C3177-215	17,154	51,462	56,530
C3177-223.5	13,975	41,925	46,590
C3177-242	1,600	4,800	8,570
C3177-251	15,968	47,904	53,170

Appendix C

Mineralogy of Borehole C3177

Appendix C

Mineralogy of Borehole C3177

This appendix contains a letter report about the mineralogy of samples from the first Immobilized Low-Activity Waste (ILAW) borehole C3177 (299-E17-21). The report is titled *Mineralogy of Selected Sediment Samples from Borehole 299-E17-21* and was written June 30, 2000.

.

Mineralogy of Selected Sediment Samples from Borehole 299-E17-21

S. V. Mattigod, R. J. Serne, R. E. Clayton, T. Schaef, and D. McCready

June 30, 2000

Introduction

Previous Hanford operations involving production of fissionable materials resulted in large quantities of liquid waste. These wastes are currently stored in underground storage tanks. The Office of River Protection (ORP) is planning to vitrify and store the immobilized low-activity wastes (ILAW) in a shallow burial facility in 200E area of the Hanford site. The acceptance of this disposal scenario, depends largely on reliable assessment of mobility of contaminants from the storage facility and their impact on the environment. The essential requirements for the performance assessment of the ILAW facility have been described by Mann et al. (1998). At present, the design of the ILAW facility and an assessment of its long-term performance are being conducted by the CH2M-Hill Hanford company (CHG) with the assistance of Pacific Northwest National Laboratory (PNNL). Prediction of contaminant mobility around and beneath the disposal facility requires the knowledge of physical, chemical, and mineralogical properties of the vadose zone sediments. Therefore, to collect such data, a borehole (299-E17-21) was drilled at the southwest corner of the proposed ILAW site, and sediment samples were collected. The geological data collected from this drilling activity has been published by Reidel et al (1998) and Reidel and Horton (1999). The determination of physical and chemical properties of the sediment samples from borehole 299-E17-21 have been completed by Fayer et al. (1998). The chemical properties of these sediments namely, pH, CEC and distribution coefficients for selected radionuclides were determined by Kaplan et al. (1998). The objective of this study was to supplement the geochemical data package for ILAW-PA by determining the mineralogical characteristics of selected Hanford formation sediment samples collected from borehole 299-E17-21.

Materials

A total of eight representative core samples from the Hanford formation were selected for analysis. These were three samples from layer 1 (24A, 31A, and 35A), three samples from layer 2 (12A, 14A, and 16A), and two samples (7A and 10A) from layer 3. The description of these core samples as provided by Reidel et al. (1998) are listed in Table 1.

The core descriptions (Table 1) showed that these samples consisted mainly of sand-size material derived from roughly equal proportions of basaltic and felsic parent materials. Many of the samples contained calcium carbonate as coatings, discrete particles, and cementitious material. Each sample was homogenized and subsamples were drawn for particle size separation.

Methods

Weighted quantities of each sediment sample were wet-sieved according to the ASTM D-422 standard method. The wet sieving was conducted with a nest of #10 (2 mm), #20 (0.85 mm), #40 ((0.425 mm), #60 (0.25 mm), #140 (0.106 mm), and #200 (0.075 mm) sieves. All material coarser than 200 mesh was composited, dried in an oven a t 110^{o} C,

Table 1. Description of Selected Core Sample from Borehole 299-E17-21.

CORE NUMBER	CORE INTERVAL (FT)	DESCRIPTION
7A	45.9 – 47.9	Medium to fine-grained sand with minor silts; sparse pebbles up to 1 inch; 50% basalt, 50% felsic. 45.9 $CaCO_3$ cementing sand into poorly consolidated nodules.
10A	57.8 – 59.8	57.8 – 58.1 Medium- to coarse-grained sand with some $CaCO_3$ 58.1 – 58.5 Cemented soil zone; fine- to medium-grained sand 58.5 – 59.8 Medium-grained sand
14A	80.3 – 82.8	Compacted medium- to fine-grained sand; some silt; 50% basalt, 50% felsic; minor $CaCO_3$ probably as grain coatings.
16A	100.5 – 103.0	Medium-grained sand; some $CaCO_3$ coating grains.
20A	129.7 – 132.2	Fine- to medium-grained sand, some silt; less than 50% basalt; some $CaCO_3$ as discrete particles and grain coatings.
24A	180.7 – 182.7	Fine- to medium-grained sand; uniform grain size; 50% basalt, 50% felsic; no bedding; well compacted, minor $CaCO_3$ cement.
31A	219.6 – 221.6	Fine-grained sand compacted by not cemented; faint bedding. 219.0 Pebbles of basalt and andesite; rounded.
35A	239.5 – 241.5	239.5 – 240.0 Granular to pebbly gravel (1/8 inch), mainly basalt; no sand matrix, open framework. 240.0 – 240.4 Grading into coarser gravel (1/4 to 1/2 inch); no sand matrix, open framework. 240.4 – 240.9 Coarse gravel with sand matrix; gravel up to 1 inch in diameter; coarse-grained sand; 50% basalt, 50% felsic.

Cooled and weighted to determine the mass of sand fraction material in the samples. The material passing the 200 mesh sieve was separated into silt (>2 μm) and clay ($\leq$ 2 μm) fractions using the hydrometer method (ASTM D-422, 1972). The silt fraction was dried in an oven at 110^o C, cooled and weighted. The clay suspension was flocculated and oriented glass slides were prepared with appropriate treatments such as ion saturation, glyceration, and heating as outlined by the procedure of Amonette (1991).

A subsample of the sand fraction of each sample was prepared for x-ray diffraction analysis by grinding in a corundum mortar and pestle. The ground material was packed into sample holders to achieve random particle orientation. Subsamples of silt fractions were packed into sample holders without any grinding for x-ray analysis. Four sample slides of each clay fraction, consisting of Mg-saturated, Mg-saturated and glycerated, K-saturated, K-saturated and heated to 450^o C were prepared to accurately identify different types of clay minerals. From x-ray diffraction data, minerals in each size fraction of the sample were identified with semiquantitative estimates of mineral mass. Based on these data, estimates of mineral content, and CEC of whole soil were computed.

Results and Discussion

Soil Texture

The particle size analysis data indicated that the sand content of these soils ranged from about 78 to 98%, the silt content varied from about 1 to 10% and clay fraction constituted about 0.6 to 7% (Table 2). The textural data showed that all the sediment samples except 10A and 14A were sands. The samples 10A and 14A had sandy loam texture.

Table 2. Particle Size Distribution of Selected Sediment Samples from Borehole 299-E17-21.

Sample #	Sand > 75 μm	Silt 75 – 2 μm	Clay < 2 μm
7A	92.1	5.5	2.4
10A	82.1	14.6	3.3
14A	79.4	13.6	7.0
16A	94.7	3.8	1.4
20A	90.0	8.8	1.2
24A	91.3	6.1	2.6
31A	88.4	10.0	1.5
35A	98.3	1.1	0.6

Mineralogy

The mineralogical composition of the sand, silt and clay fractions of the sediments are tabulated (Tables 3 – 5) and the x-ray diffraction data are included in Appendix A. About 5% by weight of corundum was detected in all sand samples which was contamination resulting from grinding the soil in a corundum containing mortar and pestle. The semiquantitative mineral contents of sand fractions therefore, were normalized to eliminate the corundum content.

The dominant minerals in the sand fractions of all samples were quartz (~66 to 82% by mass) and feldspars (~15 to 31%) (Table 3). These minerals (quartz, and anorthite and orthoclase, both feldspars) constituted approximately 92 to 99% of the total mass of the sediment samples. Trace quantities of muscovite mica, chamosite (a type of chlorite) and ferrotschermakite (an amphibole mineral) were also detected in the sand fractions (Table 3). The silt fractions of these samples were also dominated by quartz (~61 – 76%) and feldspars (~19 – 44%) (Table 4). Compared to the sand fractions, the silt fractions contained higher amounts of muscovite and chamosite (~1 – 5%), and ferrotschermakite (1 – 10%). Illitic mica, was the dominant mineral (~42 to 60% by mass) in the clay fractions of all the sediment samples (Table 5). About 14 to 17% chlorite and about 21 to 28% kaolinite were also found in clay fractions. Minor amounts (3 to 12%) of smectite (a high surface, high CEC mineral) were also detected in the clay fractions of all samples. Overall, quartz and feldspars dominated the sand fractions, whereas, the clay fractions

were dominated by illitic mica and chlorite. These size-dependent mineral distribution are typical of primary (quartz and feldspars) and secondary (illite, chlorite, kaolinite and smectite) mineral occurrence in soils undergoing chemical weathering. The mineralogy of these sediments is typical of published mineralogy of other Hanford sediments (Schramke, 1988).

Based on the mineralogy data (Tables 3- 5) and the mass distribution of particles in each size fraction (Table 2), the mineral distribution on the bulk soil basis were computed (Tables 6,7). As expected, in all samples (predominantly sandy in texture), the minerals which are dominant in the sand and silt fractions namely quartz and feldspars also dominate the mineralogy of bulk soils (~91 – 95%). All other minerals occur in minor to trace concentrations in these soils.

Although the mineralogy of these soils are dominated by quartz and feldspar minerals, other minerals such as illite, chlorite, smectite and kaolinite that have characteristics such as high surface areas, ionizable exchange sites, and specific adsorption interlayer sites significantly influence bulk soil chemical properties such as CEC. Therefore, calculations were made to assess the contribution of each mineral to the overall CEC of whole soil. The results (Table 8) show that although the minerals mica, chlorite, smectite and kaolinite together constitute only about 5 to 9 % of the total soil mass, they account for about 40 – 60 % of the total exchange capacity of the whole soils. Only trace amounts (<0.6%) of smectite were detected in these soils however, because this mineral has a very high surface area it accounts for about 4 to 17 % of the CEC of the whole soils. Also, it is well-established that minerals such as illitic mica in Hanford sediments specifically adsorb radionuclides such as 137Cs (Mattigod et al. 1993, 1994). Therefore, mica although constituting only 3 to 5 % of the soil mass would significantly affect the specific adsorption of alkali cations such as Cs and K by the whole soil.

Also, the calculated CEC of the Whole soils agreed reasonable well with the measured CEC values except in the case of samples 24A, 31A and 35A. The measured CEC values for these sample were about twice as high as the calculated values. Because the mineralogy of these sample were not significantly different from the other core samples, the anomalously high measured CEC values were attributed to the presence of trace amounts of carbonates present in these sediments.

Table 3. Semiquantitative Estimates (wt %) of Minerals Identified in Sand Fractions of Selected Sediment Samples from Borehole 299-E17-21

Mineral Group	Mineral Species	Ideal Chemical Composition	Sample #							
			7A	10A	14A	16A	20A	24A	31A	35A
Quartz	Quartz	SiO_2	82	74	66	76	76	66	74	71
Feldspar	Anorthite	$(Ca, Na)(Al, Si)AlSi_2O_8$	10	20	30	20	20	31	21	25
Feldspar	Orthoclase	$KAlSi_3O_8$	5	5	1	1	1	1	1	1
Mica	Muscovite	$KAl_2(AlSi_3)O_{10}(OH)_2$	1	1	1	1	1	1	1	1
Chlorite	Chamosite	$(Fe, Al, Mg)_6(Al, Si)_4O_{10}(OH)_8$	1	1	1	1	1	1	1	1
Amphibole	Ferrotschermakite	$Ca_2Fe_3Al_2(Si_6Al_2)O_{22}(OH)_2$	--	--	1	1	1	--	1	1

Table 4. Semiquantitative Estimates (wt %) of Minerals Identified in Silt Fractions of Selected Sediment Samples from Borehole 299-E17-21

Mineral Group	Mineral Species	Ideal Chemical Composition	Sample #							
			7A	10A	14A	16A	20A	24A	31A	35A
Quartz	Quartz	SiO_2	65	71	49	61	64	62	73	76
Feldspar	Anorthite	$(Ca, Na)(Al, Si)AlSi_2O_8$	20	14	39	31	20	19	19	20
Feldspar	Orthoclase	$KAlSi_3O_8$	5	5	5	1	1	5	5	1
Mica	Muscovite	$KAl_2(AlSi_3)O_{10}(OH)_2$	5	5	5	5	1	5	1	1
Chlorite	Chamosite	$(Fe, Al, Mg)_6(Al, Si)_4O_{10}(OH)_8$	5	5	1	1	5	5	1	1
Amphibole	Ferrotschermakite	$Ca_2Fe_3Al_2(Si_6Al_2)O_{22}(OH)_2$	--	--	1	1	10	5	1	1

Table 5. Semiquantitative Estimates (wt %) of Minerals Identified in clay Fractions of Selected Sediment Samples from Borehole 299-E17-21

Mineral Group	Mineral Species	Ideal Chemical Compositi	Sample #							
			7A	10A	14A	16A	20A	24A	31A	35A
Smectite	--	$(Ca, Mg, Na, K)_{0.33}Al_2(Al_{0.33}Si_{3.67})O_{10}(OH)_2$	8	5	4	3	8	8	12	8
Mica	Illite	$K_{0.75}Al_2(Al_{0.75}Si_{3.25})O_{10}(OH)_2$	56	60	60	59	55	51	44	42
Kaolinite	Kaolinite	$Al_4Si_4O_{10}(OH)_8$	22	21	22	21	22	26	28	25
Chlorite	--	$(Fe, Al, Mg)_6(Al, Si)_4O_{10}(OH)_8$	14	14	14	17	15	15	15	25

Table 6. Calculated Mineral Distribution on Whole Soil Basis (wt %) in Selected Sediment Samples from Borehole 299-E17-21

Mineral Group	7A			10A			14A			16A			20A			24A			31A			35A		
	Sand	Silt	Clay	Sand	Silt	Clay	Sand	Silt	Clay	Sand	Silt	Clay	Sand	Silt	Clay	Sand	Silt	Clay	Sand	Silt	Clay	Sand	Silt	Clay
Quartz	62	12	--	63	8	--	59	3	--	66	6	--	65	6	--	59	5	--	53	17	--	68	1	--
Feldspar	12	5	--	21	3	--	28	2	--	19	3	--	18	2	--	28	5	--	16	5	--	25	--	--
Mica	1	1	3	1	Tr	2	1	Tr	3	1	Tr	2	1	Tr	2	1	Tr	2	1	Tr	2	1	--	1
Chlorite	1	1	1	1	1	Tr	1	Tr	1	1	Tr	Tr	1	1	1	1	Tr	1	1	Tr	1	1	--	1
Amphibole	--	--	--	--	--	--	1	Tr	--	1	Tr	--	1	1	--	--	Tr	--	1	Tr	--	1	--	--
Smectite	--	--	Tr	--	--	Tr	--	--	Tr	--	--	Tr	--	--	Tr	--	--	Tr	--	--	Tr	--	--	Tr
Kaolinite	--	--	1	--	--	1	--	--	1	--	--	1	--	--	1	--	--	1	--	--	2	--	--	1

Table 7. Calculated Mineral Distribution (wt %) in Selected Sediment Samples from Borehole 299-E17-21.

Mineral Group	7A	10A	14A	16A	20A	24A	31A	35A
	Wt %							
Quartz	74	71	62	72	71	64	70	69
Feldspars	17	23	30	22	20	30	22	25
Mica	4	3	4	3	3	2	3	2
Chlorite	3	2	2	1	3	2	2	1
Amphibole	--	--	1	1	2	Tr	1	1
Smectite	Tr	Tr	Tr	Tr	Tr	Tr	Tr	Tr
Kaolinite	1	1	1	1	1	1	2	1

Table 8. Comparison of Calculated and Measured CEC Based on Mineralogy of Selected Sediment Samples from Borehole 299-E17-21

	7A			10A			14A			16A			20A			24A			31A			35A		
Mineral Group	Wt%	Calc CEC (meq)	% Total CEC	Wt%	Calc CEC (meq)	% Total CEC	Wt%	Calc CEC (meq)	% Total CEC	Wt%	Calc CEC (meq)	% Total CEC	Wt%	Calc CEC (meq)	% Total CEC	Wt%	Calc CEC (meq)	% Total CEC	Wt%	Calc CEC (meq)	% Total CEC	Wt%	Calc CEC (meq)	% Total CEC
Quartz Feldspar Amphibole	91	1.82	40.9	94	1.88	53.4	93	1.86	49.6	95	1.90	59.9	93	1.86	48.1	94	1.89	55.6	93	1.86	45.0	95	1.90	62.5
Mica Chlorite	8	2.00	44.9	5	1.25	35.5	6	1.5	40.0	4	1.00	31.5	6	1.50	38.8	4	1.00	29.4	5	1.25	30.3	3	0.75	24.7
Smectite	0.4	0.48	10.8	0.2	0.24	6.8	0.2	0.24	6.4	0.1	0.12	3.8	0.3	0.36	9.3	0.3	0.36	10.6	0.6	0.72	17.4	0.2	0.24	7.9
Kaolinite	1	0.15	3.4	1	0.15	4.3	1	0.15	4.0	1	0.15	4.7	1	0.15	3.9	1	0.15	4.4	2	0.30	7.3	1	0.15	4.9
Calc. Total CEC (meq/100g)		4.55			4.27			4.65			3.77			4.77			4.00			4.88			3.49	
Meas. CEC (meq/100g)		5.07			4.73			4.62			2.32			4.67			9.03			10.98			6.65	

References

ASTM D422-63. 1986. Standard Test Method for Particle-size analysis of Soils. Annual Book of ASTM Standards. American Society of Testing Material, Philadelphia, PA

ASTM D2216. 1986. Laboratory Determination of Water (Moisture) Content of Soil, Rock, and Soil-Aggregate Mixtures. Annual Book of ASTM Standards, v.4.08. American Society of Testing Material, Philadelphia, PA

ASTM D4129-88. 1988. Standard Methods for Total and Organic Carbon in Water by High Temperature Oxidation and by Coulometric Detection. American Society for Testing and Materials, West Conshohocken, PA.

Amonette, JA. 1991. Soil Mineralogical Analysis by X-ray Diffraction. Procedure JEA, Pacific Northwest National Laboratory, Richland, WA

EPA-600/R-93-100, Methods for Determination of Inorganic Substances in Environmental Samples. U. S. Environmental Protection Agency, Washington, D. C.

Fayer MJ, AL Ward, JS Ritter, and RE Clayton. 1998. Physical and Hydraulic Measurements of FY 1998 Borehole Cores. Letter Report. September 10, 1998. Pacific Northwest National Laboratory, Richland, WA

Govindaraju, K., 1994. Geostandards Newsletter. V. 18, Special Issue, p. 1-158.

Kaplan, DI, KE Parker, and IV Kutynakov. 1998. Radionuclide Distribution coefficients for Sediments Collected from Borehole 299-E17-21: Final Report for Subtask 1a. PNNL-11966. Pacific Northwest National Laboratory, Richland, WA

Langmuir, D. 1997. "Aqueous Environmental Chemistry" Prentice-Hall Inc. NJ

Mann, FM, RJ Puigh, PD Rittman, NW Kline, JA Voogd, Y Chen, CR Eiholzer, CT Kincaid, BP McGrail, AH Lu, GF Williamson, NR Brown, and PE LaMont. 1998. Hanford Immobilized Low-Activity Tank Waste Performance Assessment. DOE/RL-97-69. U.S. Department of Energy, Richland Operations Office, Richland, WA

Mattigod, SV, RJ Serne, and H Freeman, 1994. 100 Area Soil-Washing Bench-Scale Tests. DOE/RL-93-107. US Department of Energy, Richland Operations Office, Richland, WA

Mattigod, SV, RJ Serne, and H Freeman. 1994. 100 Area Soil-Washing Bench-Scale Tests on 116-F-4 Pluto Crib Soil. WHC-SD-EN-TI-268. Westinghouse Hanford Company, Richland, WA

Reidel, SP, KD Reynolds, and DG Horton. 1998. Immobilized Low-Activity Waste Site Borehole 299-E17-21. PNNL-11957. Pacific Northwest National Laboratory, Richland, WA

Reidel, SP, and DG Horton. 1999. Geological Data Package for 2001 Immobilized Low-Activity Waste Performance Assessment. PNNL-12257, Rev. 1. Pacific Northwest National Laboratory, Richland, WA

Schramke, JA. 1988. Characterization of 200 Area Soil Samples. Letter Report. September 29, 1988. Pacific Northwest National Laboratory, Richland, WA.

SW-846, 1986. Test Methods for Evaluating Solid Waste: Physical/Chemical Methods. Third edition. U. S. Environmental Protection Agency, Office of Solid Waste and Emergency Response, Washington, D. C.

Distribution

No. of Copies

ONSITE

4 **DOE Office of River Protection**
- C. A. Babel H6-60
- P. E. LaMont H6-60
- DOE Public Reading Room (2) H2-53

5 **CH2M Hill Hanford Group, Inc.**
- K. C. Burgard L6-57
- A. J. Knepp H6-60
- F. M. Mann E6-35
- D. A. Myers E6-35
- G. Parsons L6-75

2 **Flour Federal Services**
- R. Khaleel E6-17
- R. J. Puigh E6-17

3 **Flour Hanford, Inc.**
- B. H. Ford E6-35
- G. A. Jewel A0-21
- M. I. Wood H8-44

No. of Copies

ONSITE

21 **Pacific Northwest National Laboratory**
- S. R. Baum P7-22
- C. F. Brown P8-37
- R. W. Bryce E6-35
- M. J. Fayer K9-33
- K. N. Geiszler P7-22
- D. G. Horton (2) K6-81
- C. T. Kincaid K9-33
- K. M. Krupka K6-81
- I. V. Kutnyakov P8-37
- W. J. Martin K6-81
- B. P. McGrail K6-81
- P. D. Meyer BPO
- K. E. Parker P8-37
- S. P. Reidel K6-81
- R. J. Serne P8-37
- H. T. Schaef K6-81
- M. M. Valenta P8-37
- T. S. Vickerman P8-37
- Hanford Technical Library (2) P8-55